

# ISOLDE NEWSLETTER 2021



- [Introduction](#) • [Information for users coming to ISOLDE in 2021](#)
- ISOLDE facility** • [News from the technical teams](#) • [New electron gun for REXEBIS](#)
- RIB applications** • [ASPIC and ASCII: studying 2D materials using radioactive probe atoms](#) • [Quantum colour centers in diamond studied by emission channeling with short-lived isotopes \(EC-SLI\) and radiotracer photoluminescence](#) • [Local probing  \$\text{Ca}\_2\text{MnO}\_4\$  structural phase diagram and negative thermal expansion properties](#) • [Preparing xenon samples for future medical applications of  \$\gamma\$ MRI](#)
- Ground-state properties** • [High-resolution Laser Spectroscopy of  \$^{27-32}\text{Al}\$](#)  • [A year of success at CRIS](#) • [A New laser Ablation Source For ISOLTRAP](#) • [Nuclear structure of  \$^{181}\text{Au}\$](#)
- Beta-decay studies** • [Simulation and calibration of the IDS charged-particle setup](#) • [Determining the branching ratio of the rare  \$\beta\$ -proton decay of  \$^8\text{B}\$  nucleus](#) • [Indium Energy Spectrum Shape \(InESS\) at WISArD](#)
- Studies with post-accelerated beams** • [Towards the Island of Inversion with the ISOLDE Solenoidal Spectrometer](#) • [Coulomb excitation  \$^{142}\text{Xe}\$](#)  • [Resonance excitations in the  \$^7\text{Be}\(d,p\)^8\text{Be}^\*\$  reaction up to 20 MeV](#)
- Other news** • [MEDICIS and MELISSA operation in 2020](#)
- ISOLDE Support** • [Support and Contacts](#)

[isolde.cern](http://isolde.cern)





## Introduction

*Gerda Neyens for the ISOLDE collaboration*

The year 2020 started with great promise. A refurbished cryomodule was shipped back to ISOLDE and successfully installed in the HIE-ISOLDE accelerator bunker in mid-January and in February the new Front-End (FE10) was moved from the test bench in the off-line laboratory to building 179. By the end of February all teams were on track with the many planned LS2 activities (Long Shutdown 2). Preparations were made for an operational start-up of the low-energy side of ISOLDE by the end of April, and the HIE-ISOLDE accelerators by summer 2020, thus allowing for many preparatory machine studies and stable beams for testing new equipment in the hall.

And then the COVID virus stopped all activities... Around mid March CERN went into a safe mode. All activity on site was stopped, reducing the number of people from over 7000/day to just a few hundred. Only people needed to maintain the facility in a safe mode were allowed to come (occasionally) on site. This continued until early May. Then, a gradual return of people was initiated, increasing the number of allowed persons on site by a few hundred per week, and with priority given to those that are crucial to finish the LS2 work. By early July, all persons crucial for the preparations of the CERN facilities to restart operation after LS2 (also at ISOLDE), were allowed back on site, while those that could telework remained teleworking. In September, more and more people started coming back at least a few days per week, gradually reaching around 5000 persons/day by end of October. Then, another COVID wave hit the region and teleworking again became mandatory for all those that could do so. Luckily, our technical teams could continue working on-site and also our PhD students and post-docs preparing and upgrading experiments in the ISOLDE hall were allowed to come to ISOLDE about 50% of the time. Thus, preparations continued.

Now, we have become used to a new mode of working, which has continued since. Every day about 50% of the scientists are allowed on site, while the majority of the technical staff comes almost daily. The restaurants are open, but tables are placed such that only 2 persons can sit per table, with a 2 m distance (and the same outside). Thus, social life is very limited, as everywhere in the world.

During last year, stable beams were successfully produced in the new FE10 and delivered through the GPS magnet towards several beam lines. Stable beams were also produced with the REX ion source, the new REX-EBIS electron gun was successfully commissioned, and beams were accelerated in the refurbished HIE-ISOLDE accelerator with improved transmission thanks to new diagnostic boxes installed throughout the machine. Successful beam commissioning of the full REX/HIE ISOLDE facility using stable beam from REX and GPS (FE10) was carried out in 2020, but some of the foreseen extensive machine studies could not be scheduled due to the 10 weeks delay caused by the COVID shutdown. However, numerous studies were achieved anyway, including tests of many new pieces of hardware in the low- and high-energy sides of ISOLDE (e.g. new scanners and Faraday cups, new beam diagnostics and Si detectors, etc...). In April 2021, the final parts were commissioned: beam from the new FE11 was sent through IS-COOL with more than 80% transmission efficiency after initial tests. On the RILIS side, several improvements have been realized. It will now be possible to produce laser-ionized beams from GPS and HRS in parallel, allowing for more efficient planning of beam time. The laser equipment has been upgraded and access to the full spectral range has been significantly improved.

Now the full ISOLDE is ready to be handed over to the operations team, and to prepare for receiving

the first protons on its two new target stations towards the end of May, in preparation for producing the first radioactive beams for low-energy physics experiments on June 21. HIE-ISOLDE will provide stable beams for tests from July 7 onwards, and physics with radioactive beams will start on July 26. Protons will be available till November 15, while experiments with stable or long-lived isotopes might be scheduled afterwards. The start-up in 2022 will be earlier than usual, with protons for ISOLDE most likely available already by end of February 2022. We will look forward to having the MINIBALL detector back into operation by then, after it was used for a very successful measurement campaign at the RIBF in Japan (which was also delayed due to COVID).

This completes a more than 2 years shutdown period, during which the ISOLDE community has been very active in preparing for its future. We have had two successful EPIC workshops (the last one fully on-line) attended by more than 150 persons to discuss how we can fully exploit the potential of ISOLDE at CERN. Several ideas have been raised and are now being collected for publication in a Special Topics issue of the European Physical Journal. We welcome all of you to sign this paper. Please contact one of the corresponding authors or a member of the coordination writing team, to add your name (<https://indico.cern.ch/event/928894/page/21180-proceedings>) or if you want to contribute to the ongoing writing process (even for proof reading, compiling, etc...).

At the last ISOLDE Workshop and Users Meeting, also held fully on-line, the EPS Lise Meitner Award for Nuclear Physics was handed over (virtually) to Klaus Blaum, Piet Van Duppen and Bjorn Jonson who have shaped the ISOLDE facility and contributed significantly to its research program during the past decades (<https://isolde.cern/index.php/lise-meitner-award-awarded-k-blaum-b-jonson-p-van-duppen>).

Despite the COVID outbreak, the construction of the new laboratory for producing nano-material targets for ISOLDE could proceed as planned, and the work is fully

on schedule to reach the objective of producing nano actinide targets by the end of 2021. The infrastructure work will be finalized by early June. The ventilation of the Class A laboratory will restart then and the new Nanolab will be commissioned during the summer, after the reception of all laboratory equipment.



Figure 1: Departing ISOLDE Technical Coordinator Richard Catherall

In the ISOLDE hall, work resumed gradually during summer 2020 and the GLM/GHM areas were fully re-

built to comply to modern legislation for the manipulation of open sources. This area is now well separated from the rest of the ISOLDE hall and it will operate with restricted access: users will no longer be allowed inside this area during isotope collections or experiments. On the other side of the hall, the NICOLE cryostat is finally being removed, after COVID stopped the planned removal works in March 2020. Space has become available to install a new cryogenic Paul trap that will be connected towards the end of 2022 to a 30 keV MR-TOF (provided by the MIRACLS experiment), for preparing highly-purified RIB's for the new PUMA experiment in 2023. Potentially one other (new) experiment can be coupled to the MR-TOF (open for discussion). Finally, a new fast tape station has been installed and is currently being commissioned, in close collaboration between the target team and some of the ISOLDE fellows.

Thus, ISOLDE is ready to restart operation and we are all looking forward to a new running period, which will last until the end of 2024. Many experiments have been upgraded and new set-ups or detection systems have been developed during LS2. They will bring a lot of new physics results, in the years to come.

The year 2020 has also brought some important changes in the ISOLDE local team. After 37 years at CERN, of which more than 10 years as the Technical Coordinator of the ISOLDE facility, Richard Catherall handed over his duties to two persons: Joachim Voltaire became the new ISOLDE Technical Coordinator, while Erwin Siesling has been appointed as the ISOLDE Deputy Technical Coordinator with focus on the ISOLDE hall and HIE-ISOLDE. During 2020 they have all worked very closely together (though separated by at least 2 meters!), such that the transition has happened very smoothly and almost by itself. I would like to thank Richard, on behalf of the whole ISOLDE local team as well as all members of the ISOLDE collaboration, for his tremendous dedication to ISOLDE and for making ISOLDE the successful facility it is now. Furthermore, I want to express my personal thanks to Richard, for suggesting the name of the next big ISOLDE project: EPIC. **Exploiting the Potential of ISOLDE at CERN** is the perfect name to describe the

future for ISOLDE.

Normally, we celebrate the end of each year with a nice workshop dinner with all our collaboration members, followed by a Christmas Party with the local teams in building 508. In 2020, due to COVID, this was of course not possible. But thanks to the initiative of Ivan and Liss, our weekly Physics Group Meeting was turned into a 'Zoom Christmas party' on December 10, with a visit from Prof. Santa Klaus in person, giving us a scientific presentation about how he can distribute so many presents in such a short time all around the world, and showing us pictures of previous memorable Christmas parties. This was followed by handing over presents to each other virtually (the presents were delivered and collected in person at the Christmas tree in 508 during the days before). You can enjoy the recording of Santa's talk and some slides with photos of the Zoom meeting, at <https://cernbox.cern.ch/index.php/s/N3QaR2qrkzysp5I>



Figure 2: Prof. S. Klaus

My time as ISOLDE Physics Group Leader comes to an end in August. I would like to thank the whole ISOLDE team for their continued support, their enthusiasm and dedication. It was a real pleasure to work with all of you, members of the technical and physicist teams. You have made the previous 4 years an incredible experience for me, to which I will look back with a lot of happiness. They have been challenging years, but also very rewarding thanks to all of you. I wish all the best to Sean Freeman, who will enjoy after me this wonderful place.

Gerda Neyens, ISOLDE Physics Group Leader

## News for users 2021

Follow us on Twitter: [@ISOLDEatCERN](https://twitter.com/ISOLDEatCERN)

### ISOLDE schedule 2021 and 2022

2021 sees the start of Run3 at CERN and physics once again at ISOLDE. Protons for physics will be delivered on June 21 and will continue until November 15. Depending on the availability of services, there may be a chance of a winter physics run until early December. Low energy physics will be first with HIE-ISOLDE starting its first experiment in late July.

Beam requests for 2021 were already sent out in late 2020 and the first part of the schedule covering weeks 25 — 35 was published on 22 April. This can be found [here](#). The remaining part of the schedule will be published in the early Summer. Due to the lack of ventilation in the Class A labs in the first part of 2021, the production of new actinide targets had to be anticipated long in advance resulting in a significant re-use of 2018 units in the first part of 2021. The schedule in the first part has also relied heavily on local-based groups so that experiments can be carried out regardless of travel restrictions. It is hoped that travel will be more straightforward for the second part of this year.

A limited amount of support from the ISOLDE collaboration will be available for users who need this to attend experiments. The procedure will be similar to that adopted for ENSAR2 TNA funds. Jenny will contact the spokespeople of scheduled experiments in advance of their experiments running.

The dates for physics in 2022 will be confirmed later this year. However, as the LHC hopes to start physics in early February 2022, it should be noted that we are expecting protons to be available for physics earlier than usual next year. Protons for ISOLDE should be available from week 6 with the prospect of physics re-starting around late February. As such, beam requests for at least the first part of the running period will be sent out in Autumn 2021. More news of the finalised dates will be communicated in due course. Because of the re-

quired maintenance of the cryoplat, HIE-ISOLDE will not be available for physics until Summer 2022.

### User Access to CERN in 2021

Due to Covid-19 restrictions, at present Users are allowed to access the CERN site if their presence is considered essential for the experiment and has been approved via email by the ISOLDE Physics coordinator or the ISOLDE Physics group leader in agreement with the User's home institution. Any request should specify the reason and motivation for the visit as well as the duration and should be submitted at least 2 weeks before the foreseen arrival date.

Please note that before accessing the site, users will also need to follow the Covid-19 related instructions found on the [Users Office website](#) which includes an extra online course, a self-declaration form and CERN's strict quarantine requirements. If the user is coming from a region classed as high-risk by either France or Switzerland they must declare their planned arrival date to the CERN medical service, via [covid19.helpline@cern.ch](mailto:covid19.helpline@cern.ch), who will then decide what quarantine measures are required.

CERN has arrangements with certain hotels where users can stay if they need to quarantine, see [here](#), quarantining at the CERN hostel is not possible.

More information for Users about the CERN Covid-19 response as well as all related rules and regulations is available via [here](#).

### ISOLDE during Covid-19: running experiments

Running experiments will be different in 2021 due to the covid restrictions which will still be in place at ISOLDE. The number of people who may be present in a room/office at any one time is strictly controlled. The ISOLDE control room will be reserved primarily for the operations team and users will not generally be present in the control room. Instead, the old control room will be upgraded with modern workstations and

the ISOLDE DAQ room will be equipped with a terminal which will permit operation, beam tuning and observation. In addition, remote monitoring of the ISOLDE facility will be available so that experts situated locally and further afield can assist with the online runs. As a guide: 4 people can be accommodated in the ISOLDE DAQ room; 6 in the ISOLDE visitors room and 1 — 2 in the old ISOLDE control room.

The visitors area in B. 508 is now equipped with a high quality webcam so that zoom meetings can be held and to facilitate remote participation in experiments. Users are encouraged to avail of the CERN "Mattermost" platform where dedicated channels are in place for ISOLDE and where additional channels can be added for experiments and collaborations. The home page for the ISOLDE channels can be found [here](#).

### Proximeter

For stays longer than three days on-site, the use of the new CERN Proximeter is mandatory for all people at CERN. The proximeter records location interactions if the 2m distance limit is breached and keeps a record of such interactions for 15 days assisting track and trace searches in the event of a positive Covid-19 diagnosis. The proximeter can be reserved [here](#). As with dosimeters, colleagues can also pick up the proximeter on somebody else's behalf. They should be returned to B. 55 following your stay. An e-learning module which is recommended, although not mandatory, can be found [here](#). The proximeter will be mandatory on-site until the pandemic is over.

### INTC meetings in 2021

The INTC meetings in 2021 are as follows:

- 67th meeting of the INTC
  - June 23 and 24. This meeting is for all types of physics proposals and will be held remotely: using Zoom. Deadline for proposals is May 12 2021.
- 68th Meeting of the INTC
  - November 9 and 10. This meeting will accept proposals for High and low energy

physics. It is not yet known if it will be held as usual on the CERN site. The deadline for proposals is 28 September.

### User registration for 2021

A full description of the procedure for registering at CERN is given below. Visiting teams should use the pre-registration tool (PRT) to register new users. As in 2020: the teamleader and deputy teamleader who sends the information via PRT must have a valid CERN registration. This also applies to paper forms which have been signed at the visiting institute. Please register under "ISOLDE" rather than a specific experiment. If the teamleader or deputy do not have a valid registration, the users office will refuse to accept the documents.

### Access to ISOLDE

Access to ISOLDE is now entirely managed through [ADaMS](#) (Access Distribution and Management System). The access permission required for ISOLDE is **ISOHALL**. Once submitted it will be sent for approval to the physics coordinator where training ranks will be checked before access is granted.

### Required training courses for access to ISOLDE hall and chemical labs

All training is now accessed via the [CERN training hub](#). There are a variety of training courses required before access to the ISOLDE hall can be granted. These are divided into hands-on courses, which take place at the CERN training centre in Preveessin, and on-line courses which can be taken via the CERN online training.

There will be a change in the hands-on training courses for ISOLDE users in 2021. The radiation protection course will be given by a new trainer (based at CERN) and the electrical awareness course will be replaced by a new course which will eventually be obligatory for all users: "Electrical Safety - Working in EP experiments". The courses will run as usual on a Tuesday with the Electrical safety taking place in the morning and RP hands-on training following this. The exact timing and structure of the courses are still being finalised but will be ready for the physics period. The electrical

course will be soon available in the training catalogue. Before the new training courses are available it will still be possible for the physics coordinator to offer these courses on-demand.

Enrollment for courses should take place for these courses in advance of coming to CERN; in the event that a user is not yet registered an email can be sent to safety training: [safety-training@cern.ch](mailto:safety-training@cern.ch). However, once registered it will be still necessary to register for the hands-on courses in EDH in order to validate the training.

- Pre-requisite online training courses (can be followed prior to arrival at CERN)
  - Mandatory courses for everybody at CERN:
    - \* Emergency evacuation
    - \* Radiation Protection - Awareness
    - \* Safety at CERN
    - \* Computer Security
    - \* Covid-19 training
  - Additional courses for ISOLDE users:
    - \* Electrical Safety Awareness - Facilities
    - \* Electrical Safety Awareness - Fundamentals
- Required hands-on courses
  - Electrical Safety - Working in EP experiments
    - \* Course code: STELS03C (covid-19 version), STELS03I (post-Covid)
  - ISOLDE - Experimental Hall - Radiation Protection - Handling
    - \* Course code: STIRP06I
  - B. 508 chemical labs: The laboratories on the ground floor of 508 where solid state physics perform chemistry also have their own access. It is required to follow the online LMS course "Chemical Safety Awareness" before requesting the permission **ISOCHEM**

for 508 R-002 and **ISOEXP** for 508 R-008 for the measurement area.

- ISOLDE Traka Box: the ISOLDE TRAKA box is now integrated into Adams. To request access to the box it is necessary for users to ask for the "0508K1-002" permission in Adams.

## Visits to ISOLDE

**Note that visits to the CERN site are currently suspended until at least the end of June 2021.** The possibility of a "remote" visit via video conference exists for those brave enough. Once CERN returns to a more normal mode of operation, visits to ISOLDE are expected to be still possible. A typical visit consists of an overview presentation in the visitors' area in building 508 and – when possible – a tour of the ISOLDE facility itself along the pre-arranged visit path. In the event of a machine intervention or a conflict with physics which happens to be running, the tour of ISOLDE may be cancelled, and one remains in the 508 gallery area. Please note that weekend visits of groups are no longer possible and are not advised for individuals except in exceptional circumstances.

All visits are coordinated by Dinko Atanasov ([dinko.atanasov@cern.ch](mailto:dinko.atanasov@cern.ch)) and he should be contacted well in advance with your wishes. More details can be found on the area of the ISOLDE website [dedicated to visits](#).

## ISOLDE Publications and open access

ISOLDE should be mentioned in the abstract of articles related to experiments performed at the facility and, if possible, the ISOLDE team should be mentioned in the acknowledgements. Experiments which have benefited from ENSAR2 funding at ISOLDE should also mention this in the acknowledgements of any articles which emerge and which should echo the following: *This project has received funding from the European Union's Horizon 2020 research and innovation programme under grant agreement No 654002.* Furthermore, please note that **all** publications which have received ENSAR2 funding need to be available as open

access. This can be either green or gold but at the very least green open access will be expected of all publications which have received EU funding. Green open access can be fulfilled by submitting a manuscript copy of a paper to the library following publication.

There has been quite a lot of development regarding open access at CERN. New agreements have been signed with numerous publishers. In many cases publication costs will be covered centrally at CERN if there is at least one CERN-affiliated author in the author list. In the cases of the IOP and the APS publication costs can be covered even without a CERN author as long as the ISOLDE collaboration and IS number are mentioned e.g. "CERN, ISOLDE Collaboration, ISXXX" in the collaboration field of the submission form, and this should be added to the paper itself.

Detailed information on the open access policy and the list of agreements in place can be found on the newly revamped CERN Scientific Information Service [website](#). A guide to choosing the best option for publishing an article as open access through CERN can be found [here](#). In case of any further questions, authors can ask the experts in the CERN library questions via email: [open-access-questions@cern.ch](mailto:open-access-questions@cern.ch).

### Publications on CDS

It is increasingly important that papers from ISOLDE have proper visibility at CERN. To facilitate this, there is a specific area of the CERN Document Server from which all ISOLDE spokespeople and contacts will be able to upload DOI links (and extra information if required). Once you have signed in with your CERN credentials, you should be able to upload any new articles or theses. The link can be found <http://cern.ch/go/9lbw>. If there are any problems with uploading, please contact the physics coordinator. **A preprint of an article can also be uploaded to this area satisfying open access requirements for projects which have received TNA funding from ENSAR2.**

### Safety in the ISOLDE hall

As part of the CERN-side Covid-19 measures, working in the ISOLDE hall is subject to additional safety measures. The wearing of masks within CERN

buildings is mandatory: standard surgical masks are available for all users, and FFP2 masks are available on request. The preservation of social distance to >2m will be required at all times. Alcohol-gel dispensers have been installed throughout the CERN site and in the ISOLDE hall. Tools and workspace have to be cleaned before and after working with them. The hand-foot monitors are to be used, but one should disinfect your hands after use.

The wearing of safety helmets and shoes is mandatory inside the ISOLDE hall. It is also mandatory to check yourself on the hand-foot monitor before leaving the ISOHALL zone.

Once within the ISOLDE hall you have at your disposal additional RP protective equipment such as gloves and contamination monitors to ensure your safety. These are located in the cupboard close to the old control room. A new suite of PPE for electrical investigations can now be found close to the IDS setup in the ISOLDE hall.

A variety of "expert" courses are available for those required to perform more demanding operations such as those involving cryogenics, using the crane and lasers. Please ensure that you have followed these courses before performing these tasks.

The mechanical workshop in building 508 is fully operational. If you wish to use it a document will need to be provided which is signed by your team-leader, yourself, and our workshop supervisor, authorising you to use the selected machines in the workshop. For more information, please contact your experiment spokesperson, local contact or the coordinator.

The list of contacts for safety both for local experiments and visiting setups can be found via <https://isolde.cern/safety>. All visiting setups should ensure that they have had a safety inspection before their experiment starts at ISOLDE. Please allow sufficient time for this to be done. You can contact me for more information to prepare for this.

### Removal and shipping of equipment from the ISOLDE hall.

All equipment which has been in the ISOLDE ex-

perimental hall requires a control by radiation protection before it can be transported elsewhere or back to home institutes. A new “buffer zone” has been installed in the ISOLDE hall (close to the SAS and the HIE-ISOLDE

tunnel) which implements the CERN-wide TREC system to ensure that all controlled equipment has traceability. This is now incorporated into the EDH flow for all transport requests from the ISOLDE hall.

# ISOLDE facility

## News from the technical teams

*Reinhard Heinke, Bianca Reich, Laura Lambert, Yago Nel Vila Gracia, Francisco Josa, Edgar Reis, Mia Au, Katerina Chrysalidis, Bruce Marsh, Georgios Stoikos, Ralitsa Mancheva, Simon Stegemann, James Cruikshank, Stefano Marzari, Razvan Lica and Sebastian Rothe for the SY-STI RBS and LP sections*

### 1 Installation of new Frontends

During the long shutdown 2 (LS2) we were tasked with replacing the previous generation of ISOLDE target stations, also known as Frontends (FE). The previous generation was installed in 2010 and due to aging and high level of radiation, the expected lifetime of the FE is typically 7 years. This presented a unique opportunity to upgrade its design, performance and reliability over the long shutdown.

The new generation of Frontend (FE10) for the GPS was installed in September 2020, figure 1. It is now providing stable beam for the commissioning of the ISOLDE beamline.



Figure 1: Members of the installation team in the GPS Faraday cage

<https://isolde.web.cern.ch>

The HRS Frontend (FE11) installation is ongoing, as shown in 2, it has already been installed in its dedicated Faraday cage. The installation is proceeding on schedule and is undergoing a final investigation of its alignment to the separator magnet. The HRS FE will begin its off-line test in the second week of March and begin to provide stable beam to ISCOOL commissioning and to the ISOLDE beamlines later on.

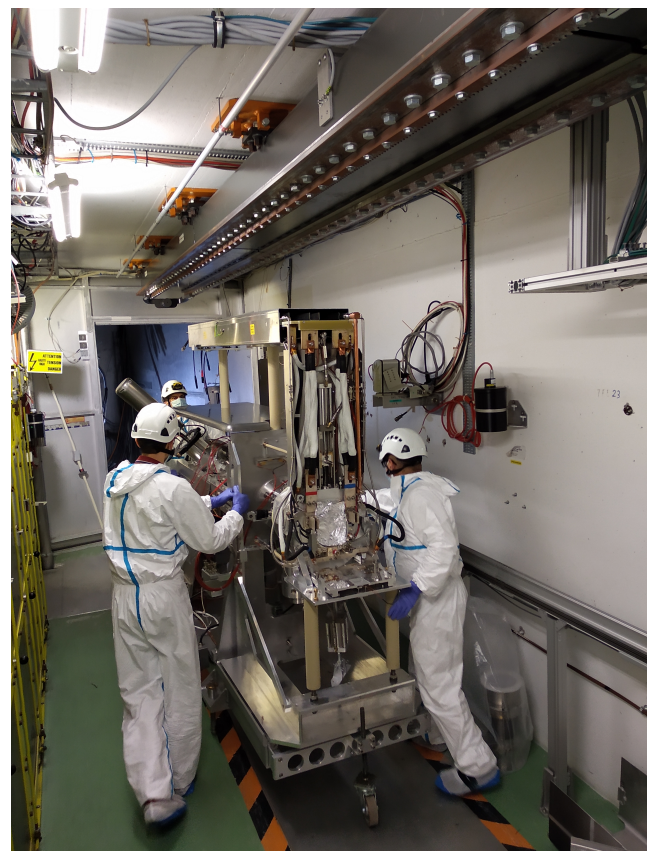


Figure 2: Transport of FE11 to the HRS faraday cage

## 2 Gas system upgrades

Supply of gases to the ISOLDE targets at a controlled concentration and rate is required to promote molecule formation through addition of reactive gasses, or act as a buffer gas in the FEBIAD type or plasma ion sources sources (VADIS, VADLIS, COMIC, or Helicon), where it is also used to monitor the ionization efficiency. The installation of the new GPS and HRS Frontends (FE10 and FE11) at ISOLDE, gave us the opportunity to upgrade the gas supply system to the target. Both Frontends are now equipped with three gas lines which can be independently coupled to the target and ion source unit. Therefore, an upgraded ISOLDE target gas system has been designed and built (see Fig. 3, EDMS: 2492542), which can be controlled remotely and it will be ready to feed these independent gas lines. The system is able to handle inert and noble gases ( $\text{Ar}$ ,  $\text{N}_2$ ), oxidizing gases ( $\text{NF}_3$ ,  $\text{O}_2$ ) as well as other gases such as  $\text{SF}_6$ ,  $\text{CF}_4$ , Air, and  $\text{H}_2$  (2% in argon). The pressure inside the gas system ranges from -1 bar up to 1.5 bar gauge. In parallel, an ATEX compliant gas system is under assessment to further upgrade the new gas system and allow the handling of CO in a safe manner.

calibrated leak, which controls the gas injection in the target.

- Loop operation, used for gas purification and improved mixing as well as for the carbonyl metal extraction system [1].

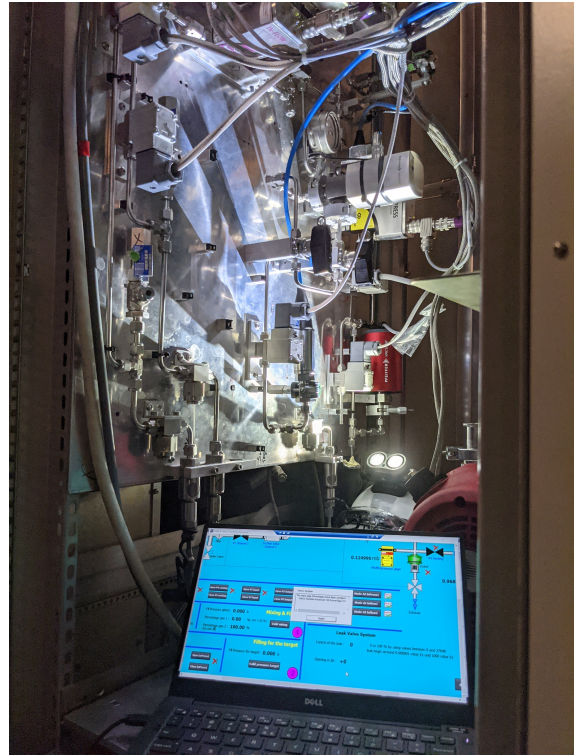


Figure 4: Photograph of the ISOLDE GPS Gas System during installation and testing.

The first gas system prototype has been successfully built and it is currently undergoing electronic tests by BE-CEM to verify its functional specifications before installation at the GPS high voltage platform. Two additional, identical systems will be constructed for HRS and Offline 2.

## 3 New detectors for the ISOLDE Tapestation

The ISOLDE tapestation is the prime piece of equipment to perform the target yield checks and optimizations, as well as beam development tasks. It uses a tape system which allows the removal of activity from the implantation point and the transport to different detectors - up to now beta counting and gamma spectroscopy were employed. After the removal of the

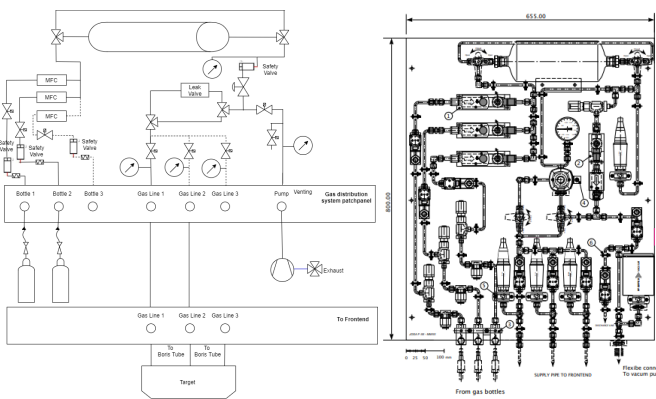


Figure 3: Left: Schematics of the ISOLDE GPS Gas System. Right: 2D design drawing.

The gas system features 3 different modes of operation:

- Calibrated leak operation or standard operation, where the system is filled with different gases up to a desired pressure.
- Leak valve operation, suitable for targets with no

previous TapeStation, which has served ISOLDE for decades, from the central beam line, the new TapeStation was moved to its final location from LA2 where it was first commissioned during 2018 ISOLDE operation. The TapeStation detection system was recently upgraded with new beta detectors based on silicon photomultiplier (SiPM) 3x3 arrays developed at IFIN-HH, Romania [2] with integrated amplification offering a low dark current and specifically designed to be operated at high counting rates ( $\sim 1$  MHz). The SiPM cells employed are the 6x6 mm C-series manufactured by Sensl. The signals originating from the 9 cells are summed, filtered and amplified using low-power operational amplifiers which output two signals proportional to the amount of light collected: fast (15 ns rise time, 100 ns decay time) and slow (100 ns rise time, 2  $\mu$ s decay time). The fast signals are sent to the ISOLDE counters and the slow signals will be digitized to extract the beta particles energy spectrum.

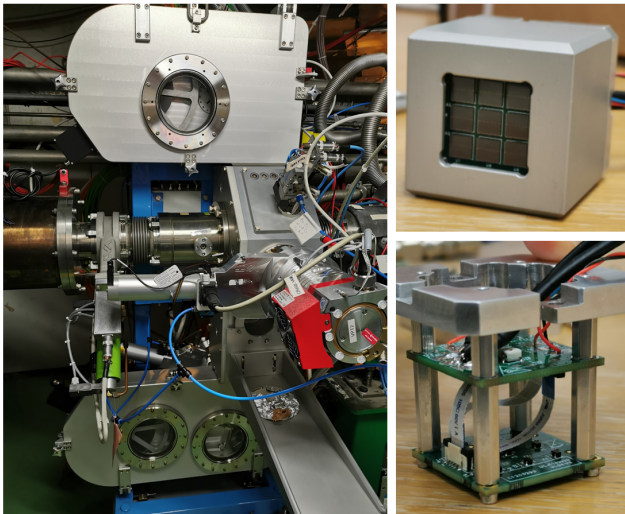


Figure 5: (left) The Fast TapeStation installed at the CA0 beamline and (right) the new compact beta detectors based on 3x3 SiPM arrays [2] coupled to 3 mm thick EJ200 plastic scintillators.

The SiPM arrays will be coupled to a 23x23x3 mm EJ200 plastic scintillator suitable for detecting beta-particles in the range of few tens of keV and up to one MeV, and tag on the beta-particles of higher energies which deposit only a part of their energy in the thin scintillator. In addition to the beta detectors, gamma-ray detection will be provided by the newly reconditioned Canberra HPGe detector used previously at the old Tape-

Station. The DAQ system is chosen such that alpha detection using a Si pad detector can be easily implemented at a later stage. The detectors will be placed in the following configuration:

- Position 0 (implantation position): one beta detector located behind the tape in the forward direction relative to the beam.
- Position 1 ( $4\pi$  beta detection): two beta detectors facing each other with the tape passing in-between, offering the best geometric coverage of almost  $4\pi$ . The detection system is surrounded by a thick Pb shielding to minimize the radiation background.
- Position 2 (beta-gamma detection - design phase): one beta detector facing the HPGe detector with the tape passing in-between, offering the possibility of beta-gamma coincidences reducing the background.
- Position 3 (alpha detection - design phase): one Si pad detector facing the implantation spot on the tape.

A new data acquisition system able to instrument all the detectors listed above was installed, based on the CAEN DT5725S with 14-bit resolution and 250 MS/s sampling rate, well suited for mid to fast signals, as the ones coming from scintillators coupled to PMTs or Silicon Photomultipliers, but also for high precision detectors such as Silicon or HPGe, coupled with charged sensitive pre-amplifiers. The previous Canberra system will be used while a deeper integration of the CAEN system into the CERN data acquisition is being developed.

## 4 RILIS

The demand for laser ionized beams at ISOLDE has risen steadily during recent on-line campaigns. Providing well above 60% of the ISOLDE ion beams has only been possible due to the continuous upgrade of the RILIS laboratory control system [3, 4].

## New laser shutters for RILIS

One of the main advantages RILIS provides, is the simple way of determining the isobaric background contamination, by performing laser on/off measurements during the initial setup of the laser ion source and also performed by the users during the experiments.

Recently, a new operational mode for the laser shutter system has been under development (see Fig. 6) and is currently undergoing testing during the ISOLDE commissioning phase. Formerly, only one shutter was available, which was solely controlled by a TTL signal, with no feedback concerning its state. The current system is remotely controlled via a newly developed software interface. A feedback shows if the shutter is open or closed, so that malfunction of the shutter can be excluded during trouble shooting. Additionally, the system has been expanded to a total of six shutters, giving the possibility to block each laser beam individually, or in any combination. A user tutorial will be provided in the beginning of May and will remain available online.

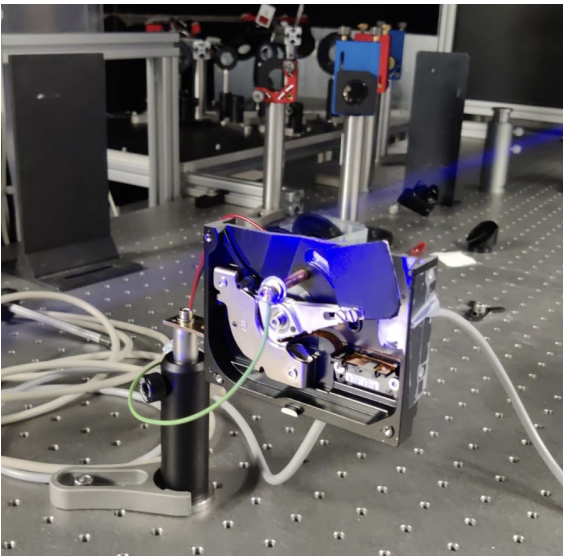


Figure 6: One of the new RILIS laser shutters during commissioning

## A Laser ion source at Offline 2

At the new laser laboratory of Offline 2 (YOL2) (see ISOLDE newsletter 2020, [5]), preparations for the first laser ionised beams are on-going. The newly developed Raman laser [6, 7] has been installed for thorough testing of broad-band and single-mode operation

of the laser system. Especially for high-resolution spectroscopy using the PI-LIST, the single-mode Raman laser will play a vital role. It provides a significant improvement of the RILIS laser system's laser linewidth capabilities and it is foreseen to be used at ISOLDE during the 2021 on-line campaign. A schematic layout of the laser table is shown in Fig. Fig. 7.

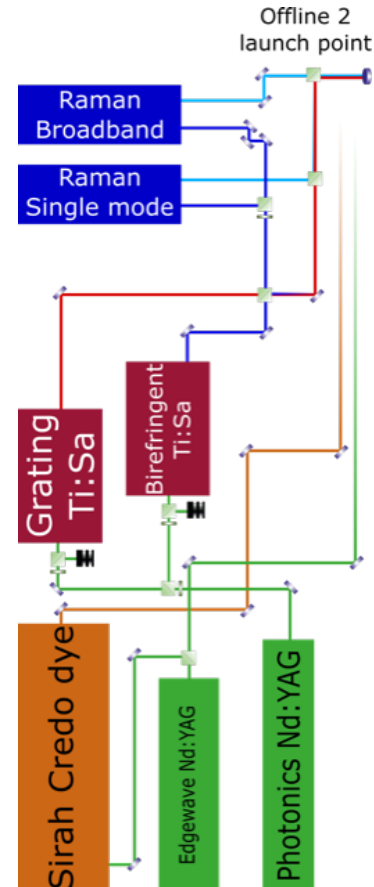


Figure 7: Layout of the laser installation at the Offline 2 facility.

## Investigation of UV induced carbon deposits

Another operational constraint during past on-line periods has been the build-up of UV induced carbon deposits on the optics transporting these laser beams. This required regular intervention for cleaning the optics and led to downtime of the laser system. A systematic investigation was launched into this matter and it has been discovered that the build-up is caused by one of the solvents used for preparing the laser dyes. Seeing as the strength of the RILIS laser system lies in its versatility for providing not only the Titanium:sapphire laser spectral range but also the dye laser one, a va-

riety of options is now under consideration to reduce and, if possible, eliminate the air contamination caused by the solvent.

## 5 LIST for Run 3

Following its last on-line application in 2018, ISOLDE's high purity laser ion source LIST has gained more attention from experiments to be exploited for clean radioactive ion beams in the near future. For the upcoming Run 3, already two experiments and two letters of intent (requesting ytterbium [8], thallium [9], polonium [10] and actinium [11]) were approved for cases where strong isobaric contamination of easily surface-ionizable elements are present. The LIST circumvents this problem by spatial separation of atomization and vaporization in the standard hot cavity ion source geometry, and element-selective laser ionization in an adjacent RFQ structure [12].

During LS2, both GPS and HRS Frontends have been equipped with new RF delivery infrastructure to supply a MHz frequency with amplitudes up to a few 100 V to the source. Whereas the previous version was limited to only one RF supply line and subsequent amplification/phase splitting by a radiation hard resonance circuit, mounted directly to the target unit, the new design allows for placing all required RF supply parts on the supply racks of the HT platform and delivering the two phases independently via two lines. This significantly facilitates both manufacturing and storing of the LIST units without the additional circuit box, as well as monitoring and manipulation of the applied voltages. As a bonus, this will also reduce the costs for waste disposal.

Two modes of RF supply have been tested in a mock-up assembly. Firstly; the previous system with the resonance amplification can still be used by placing the circuit on the HT platform before the supply lines. Secondly; a MHz DC voltage switching unit similar to the design for TRIUMF's IG-LIS ion source [13] has been constructed by Mainz University and proven

to supply sufficient voltage at manageable power consumption levels. Both options also provide the opportunity to easily apply an additional DC voltage offset to the unit, further broadening the versatility of the LIST: An electric field configuration more beneficial for efficient extraction can be realized, ions created on a different potential are transmitted on a different trajectory through the mass separator than isobaric contaminants ionized in the atomizer, and within constraints even a mass-selective RFQ transmission can be applied [14].

The custom-made radiation-hard copper waveguides (end parts of the RF supply at the Frontends), have been optimized further and were tested with aid of SY-RF-FB to better comply with impedance requirements, and routine diagnostic procedures using a vector network analyzer connected on the HT platform for target coupling and general system inspection have been established.

An important milestone towards operation of the PI-LIST for high resolution in-source laser spectroscopy [11, 15, 16], requiring off-axis passage of a laser beam through the separator vacuum chamber into the ion source region, has been addressed recently: a new extraction electrode tip with an adapted design featuring four lateral bores was installed at the GPS Frontend (see Fig. 8).

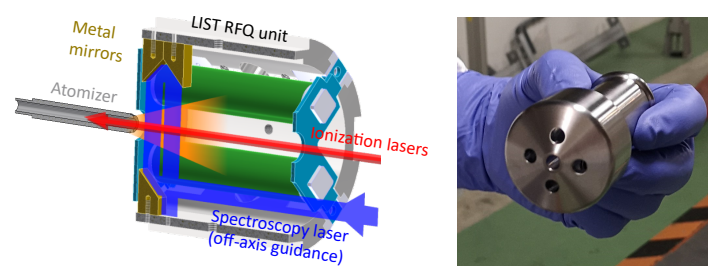


Figure 8: The PI-LIST with perpendicular laser geometry for reduction of the effective spectral Doppler broadening. Off-axis passage of a laser beam through the separator requires the shown adapted extraction electrode design.

First comparative investigations show no apparent deviation in ion beam shape and quality in this new setup for a surface ion source (see Fig. 9). These results indicate that the design change will be transparent to standard ISOLDE operation and the new electrode can remain in the machine, ready to be used for the PI-LIST.

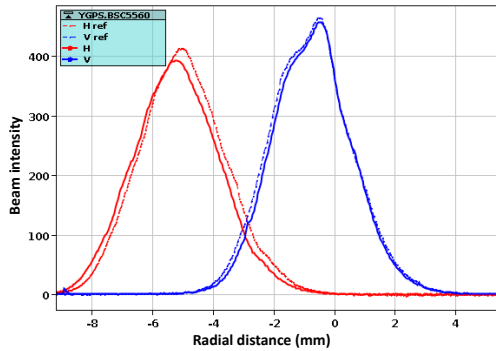


Figure 9: Ion beam scanner images taken at ISOLDE GPS. No significant deviation between the extraction electrode variants is apparent.

Further extensive testing of the LIST and PI-LIST will be performed at the Offline 2 separator, which is currently also being equipped with a replica of the new ISOLDE Frontend RF delivery system, and narrow bandwidth laser infrastructure to perform high resolution laser spectroscopy experiments.

## 6 Status of the actinide Nano Lab



Figure 10: Above: Nano Lab start and middle of construction phase one. Below: Nano Lab extension up-to-date photo.

With construction having started in the spring of 2020, the new Nano Laboratory (Nanolab) is well on its way to reach the goal of producing nano actinide target materials by the end of 2021. Regardless of the global public health crisis, the Nanolab construction was able to move forward without delays and the civil engineer-

ing is now complete with a full extension to building 179 now in place, see Fig. 10 below.

At the beginning of January 2021, the ventilation of the Class A Laboratories was interrupted, allowing for the full upgrade extension of the ventilation system into the Nanolab. This work is ongoing, with the ventilation cut expected to finish at the end of May.

Five gloveboxes have been purchased which will be used to safely handle the actinide nano materials. Four out of five of these gloveboxes will exist in a fully connected custom design residing in the oxide laboratory allowing for materials to flow more freely between the gloveboxes resulting in a more efficient and safer working environment. This customized layout, seen in Fig. 11, will allow for the entire process starting from weighing initial materials, to grinding down and producing nano slurries, and ending in nano pellets to exist all without the requirement to shuttle materials in and out of gloveboxes using lengthy bag-out procedures. The fifth glovebox will sit in the carbon lab with a custom antechamber allowing for the simple transfer of a full target assembly into and out of the glovebox. The design phase for all five gloveboxes is nearing completion with the manufacturing stage planned to start in March.

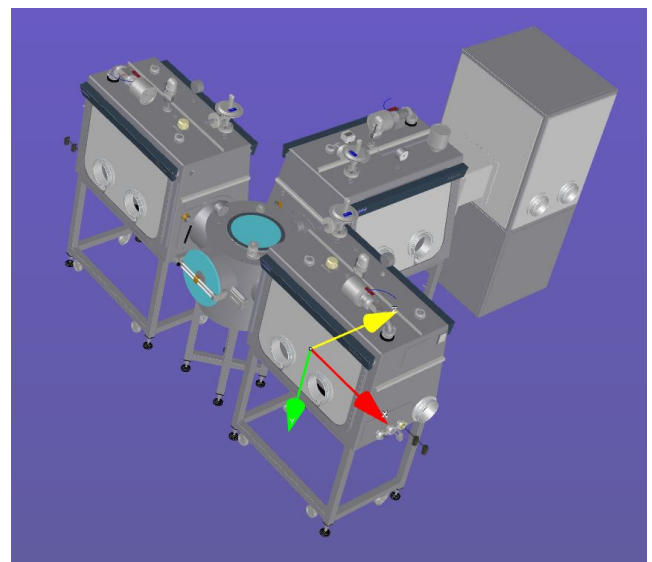


Figure 11: Custom design of four gloveboxes for the oxide-Nano laboratory.

A fumehood has also been purchased for the nano-oxide laboratory which will allow for consistent quality control tests of the nano materials. The design phase

is nearing completion with expected delivery middle of April.

## 7 Target material development

The completion of the new actinide nano laboratory will launch the production and process optimization of nano-UC<sub>x</sub> targets [17, 18], as well as other radioactive nanomaterials. Therefore, and as stated above, production of such target materials by the end of 2021 seems feasible.

Meanwhile, a campaign is on-going to transform the chemical lab in building 26 into a dedicated laboratory for production and development of non-radioactive, nanostructured target materials. Process development will be possible using a re-commissioned glove box, e.g. handling of dry nano-powders and multi-walled carbon nanotubes (MWCNTs), and a fume hood which can be used to safely handle nanomaterials in suspension. Comprehensive material characterization studies concerning micro and macrostructural target features will be enabled using a variety of different analysis techniques:

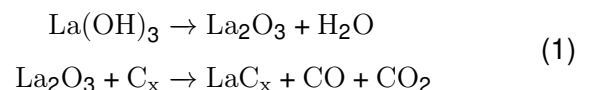
- Laser particle size analysis (particle size, particle size distribution)
- He-gas pycnometry (apparent density, open porosity)
- Gas physisorption (specific surface area, porosity, pore size distribution)
- Thermogravimetric analysis (high-temperature chemical reaction kinetics, phase transitions)
- Scanning electron microscopy in collaboration with EN-MME-MM (surface topology)

In addition, using the carburization pump stand, sintering studies of existing and new nano target materials are foreseen, to investigate the microstructural stability during target operation. The outcome will be a better understanding of target properties and operational limitations, thereby fostering a steadier on-line target performance.

In this context, the development of nano-LaC<sub>x</sub> targets has been prioritized, as they feature a two-fold benefit: firstly, compared to its micrometric equivalent that is currently in use at ISOLDE, production yields of exotic nuclei are expected to improve (e.g. <sup>100</sup>Sn), which, to date, cannot be delivered adequately to the physics experiments. Secondly, lanthanum carbides possess similar physical properties to uranium carbides such that process optimization results are directly applicable for the production of (nano-) UC<sub>x</sub> as soon as the nano laboratory goes operational.

### Towards the development of Nano-LaC<sub>x</sub> targets

Existing fabrication procedures of nano-UC<sub>x</sub> and nano-LaC<sub>x</sub> targets comprise dispersion mixing of the precursor with MWCNTs in isopropanol (IPA). New studies have been started using dichloromethane (DCM) instead of IPA, which on the one hand, potentially improves the dispersion, thus diminishing the particle size distribution. As a result, sintering effects and associated yield degradation could be mitigated during high-temperature treatments. On the other hand, it makes the process more easily adaptable to the glove box confinement conditions in the Nano Lab, as DCM is, contrary to IPA, a non-flammable solvent, therefore not leading to potential ATEX hazards.



To prove that the product is free of chlorine contamination, we are currently monitoring the carburization process of graphite-based LaC<sub>x</sub> (Eq. 1) via residual gas analysis (RGA). Preliminary results show no measurable chlorine traces after a second heating cycle (see Fig. 12, and Fig. 13). Further tests on possible Cl contamination, equivalent studies with MWCNTs and further grinding optimizations are however still required to prove the feasibility of this improvement to the existing process.

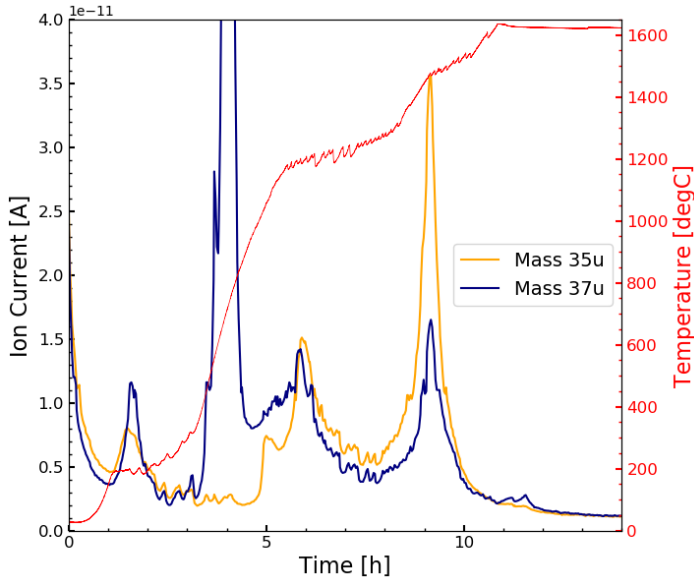


Figure 12: First carburization of the LaOH + C sample dispersed in DCM.

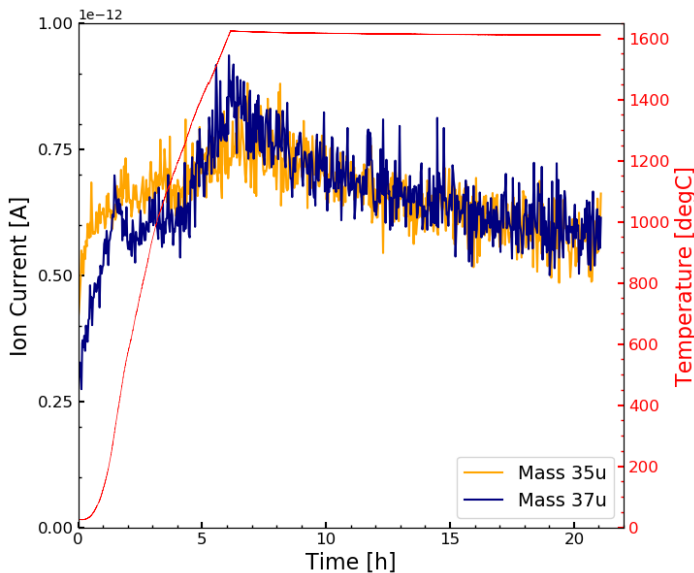


Figure 13: Re-carburization of the LaC sample previously produced

## 8 Pump stand upgrades

### Close-loop Carburization Software

Most materials used as an ISOLDE target require a heat treatment for either outgassing (e.g. zirconia fibers) or to drive a chemical reaction (e.g. carburization of uranium carbide). This heat treatment procedure is one of the several steps required for materials to be used for studies in either offline or online at ISOLDE. In this step, the material is placed in an oven, usually

a tantalum target container, which is resistively heated over a certain time using a current ramp. Especially considering exothermal chemical reactions, which release a gas like CO or CO<sub>2</sub>, it is of utmost importance to regulate the reaction speed once heating the target. Thus preventing a sudden and uncontrolled pressure increase in the system, which could lead to non-reproducible material structure and composition or, in the worst case, damage of the vacuum system.

In previous iterations, manual or open-loop systems were used to control the heating process, which either required an operator always to be vigilant while carburizing or long carburization times. Therefore, an upgraded carburization software has been implemented, which uses a compactRIO controller (Model 9054, from national Instruments) and the CERN Controls Middleware (CMW) [19]. The software acts as a reader and controller of the relevant system variables: line/target current and voltage, pressure and temperature (if there is a thermocouple inserted in the target). The voltage and pressure rates are calculated in the software to realize a more accurate control of the system. A low voltage rate indicates that the system is at steady state. After many runs carburizing materials such as CaO or La(OH)<sub>3</sub>, the control software has been proven reliable. Fig. 14 shows the frontpanel of the carburization software in operation for the carburization of a La(OH)<sub>3</sub> sample.

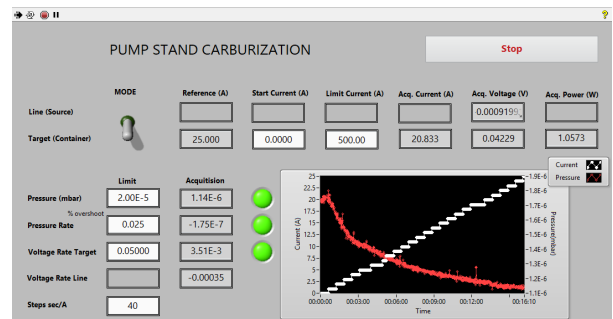


Figure 14: Frontpanel of the carburization software.

Fig. 15 shows the temperature and power plotted over time for a La(OH)<sub>3</sub> + C sample undergoing a carburization step, where the pressure limit was set to 2e-5 mbar.

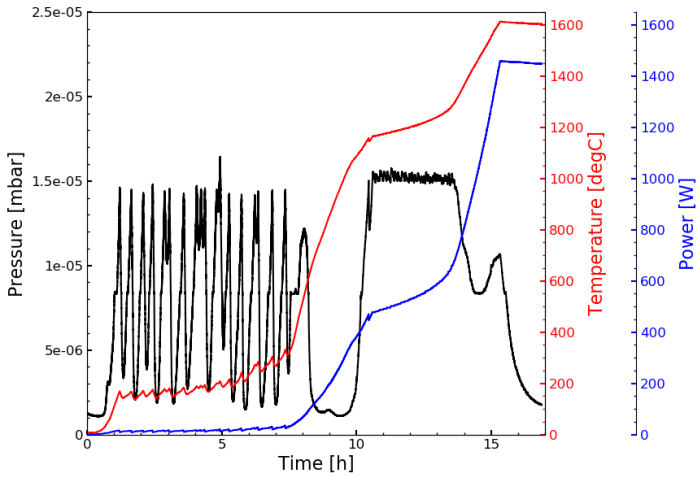


Figure 15: Pressure, temperature and power plotted over time for a carburization step of a  $\text{La}(\text{OH})_3 + \text{C}$  sample.

In addition, the pumpstand used for carburization is equipped with a residual gas analyzer (RGA type Pfeiffer Prisma), which measures the partial pressures of the elements or molecules in the vacuum chamber from mass 1 to 100 amu. Thus, it is possible to follow the chemical reactions and outgassing procedures and detect if the process behaves as expected. Furthermore, we can detect if there are contaminants present either in the sample or the chamber itself. Fig. 16 shows a waterfall plot obtained from a set of consequent mass scans obtained during the carburization of a  $\text{La}(\text{OH})_3 + \text{C}$  sample. It can be observed that there is a sudden increase, followed by a plateau, and a decrease of CO between 500 min. and 1000 min. of the experiment, which also coincides with the pressure profile of Fig. 15.

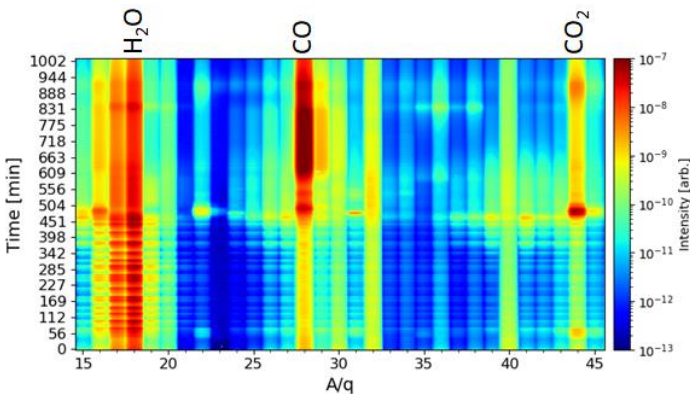


Figure 16: Waterfall plot of RGA mass scans over time. The masses for water, carbon monoxide and carbon dioxide are indicated.

## Temperature calibration application

The pump stand is also used to calibrate the temperatures of the target container and the ion source versus the applied current and heating power. Currently, this process is performed in a fully manual manner by a technician. For each measurement step a certain current is set and, after a waiting time in the order of 15 min, which is required to bring the system in an equilibrium state, the temperature is measured via an optical pyrometer. The following measurement values are recorded manually: current, voltage, pressure, observed temperature and true temperature (corrected for the emissivity of the material). In this context, we present a first version of a semiautomatic calibration software, which acquires the relevant system variables such as current, voltage, pressure and true temperature via the compactRIO-9054 controller and the CMW. Here, the user sets an initial and a final current, a desired number of measurement points and a maximum ramp speed. The calibration software (Fig. 17) controls the current ramp in the same manner as the carburization software. For each current step, once the pressure value, its derivative, and the measured drain voltage derivative are below a specified threshold, the system notifies the user, who can proceed to perform a temperature measurement via the pyrometer. The temperature is automatically read from the pyrometer and saved in a file, as well as the rest of the other relevant variables.

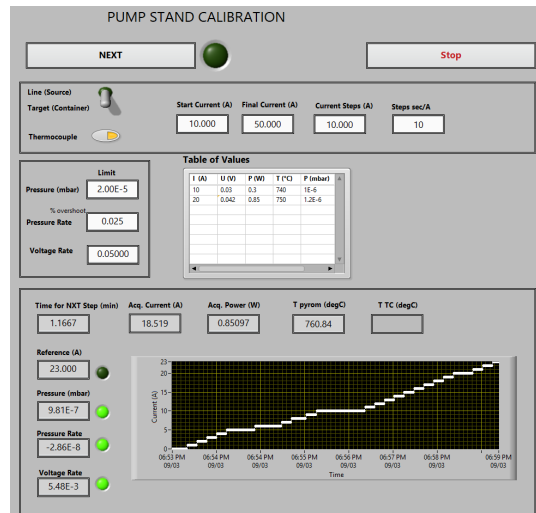


Figure 17: Frontpanel of the calibration software.

The aim is to eventually transfer the data automatically to CERN's enterprise asset management database (INFOR-EAM) that hosts all information available for the ISOLDE target and ion source units.

## 9 Molecular beams

Some elements are very difficult to deliver using the ISOL method. Refractory elements, with high melting points and low vapor pressures, often do not reach the ion source and thus cannot be produced as atomic beams. Molecular formation has been proposed as a potential solution to tackle the production of these difficult elements [20]. By forming volatile molecules in-target, refractory elements can be released to the ion source and broken up or delivered as a molecular beam [21]. Molecular beams should be stable at the high temperatures required for ion source operation, while also avoiding isobaric contaminants. With these restrictions, the challenge lies in identifying and forming the molecular species to facilitate release of a specific refractory element.

### LISA at ISOLDE

The LISA (Laser ionization and spectroscopy of the actinides) innovative training network is an EU-funded Marie Skłodowska-Curie action [22]. The LISA project aims to develop knowledge of the actinide elements, encompassing techniques for actinide production, experimental and theoretical studies of actinides and their properties, as well as their medical and environmental applications. Actinides and their isotopes are in the heavy regions of the nuclear chart, with half-lives and refractory properties that present a challenge to production and handling at ISOLDE. There is interest from the LISA program and from the scientific user community in developing the actinides as ISOLDE beams [23]. Initial studies being launched within the LISA program propose to investigate previously irradiated ISOLDE targets. These pre-irradiated targets contain an inventory of long-lived actinide species, estimated from the

proton beam they received by Duchemin et. al. [24] using ActiWiz as shown in Figure 18. Using these predicted initial inventories, the initial investigations will study both molecular extraction and laser ionization as techniques to extract actinide beams at ISOLDE.

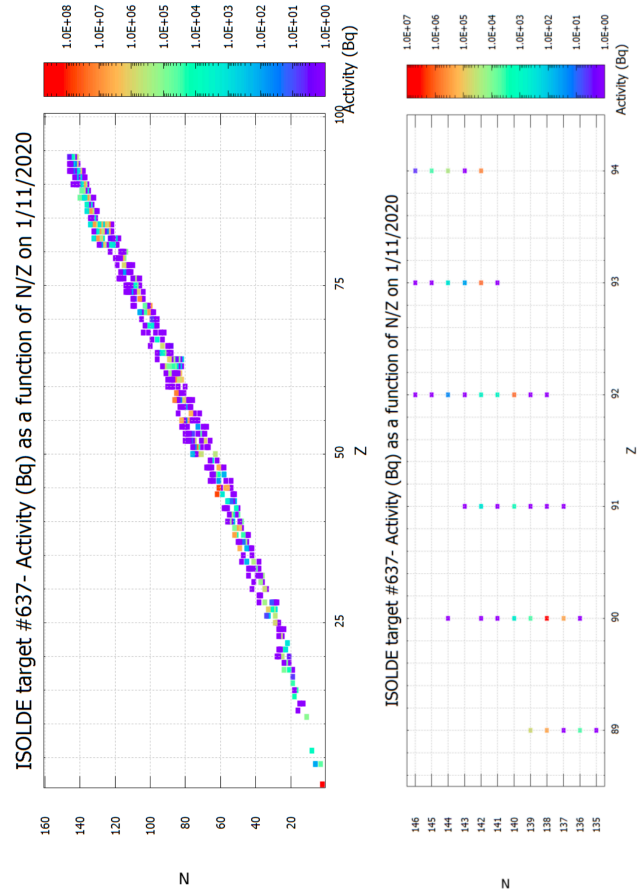


Figure 18: Radionuclide inventory and activities in target 637 on 1st of November 2020 (top picture) with a focus on actinides (bottom picture). Simulations conducted by C. Duchemin [24]

To facilitate identification of low-intensity beams of the long-lived actinides and actinide molecules, single ion counting capabilities are required for use at ISOLDE. The installation of a robust MagneToF detector (Model ETP 14925) at the GLM beamline will enable detection of exotic actinide and actinide molecular beams below Faraday cup detection levels, and for further beam identification, the teams of target and ion source development and ISOLTRAP are collaborating in the use of the ISOLTRAP MR-ToF mass spectrometer. The MR-ToF MS provides isobar mass resolution, enabling the investigation to unambiguously identify the actinide and actinide molecule beams of interest.

## Radioactive molecules at ISOLDE

Beyond developments for actinide beams and the interest in atomic beams of refractory elements, molecular beams are drawing significant interest in their own right. The letter of intent I-227 [25] was submitted to the 66th meeting of the INTC and recommended for approval, kicking off a campaign for the development of molecular beams at ISOLDE. The radioactive molecules program presents a wide range of interesting molecular beams, motivated by the potential for fundamental and applied physics research.

### Offline molecular beam developments

Initial molecular formation studies were conducted using a specifically designed molecular beam oven and ion source, presented in [5]. The design features a separately-heated reaction chamber separated thermally from the ion source heating. The design allows for control of reaction temperature and molecular formation conditions.

In collaboration with Michigan State University, we have used this setup to study the formation of beryllium molecular beams required for their batch mode ion source physics program. Beryllium is known to be a difficult element to release from thick ISOL targets. It is generally produced at ISOLDE using resonance laser ionization; therefore molecular sidebands for extraction of Be have been considered only briefly with the monofluoride, noting that on-line efficiency of  $\text{BeF}^+$  with a hot plasma source gave low efficiencies [26]. From the initial investigations, beryllium fluoride ( $\text{BeF}_2$ ) was identified as a candidate for a volatile (boiling point  $1169^\circ\text{C}$ ), high-temperature stable molecular beam. A beryllium sample was prepared and placed in the target oven. Injection of  $\text{NF}_3$  gas through a calibrated leak supplied the fluorine for in-situ molecular formation. By monitoring the temperature at the sample location and the mass-separated beam of interest, the relevant reaction temperature for in-target molecular formation can be identified.

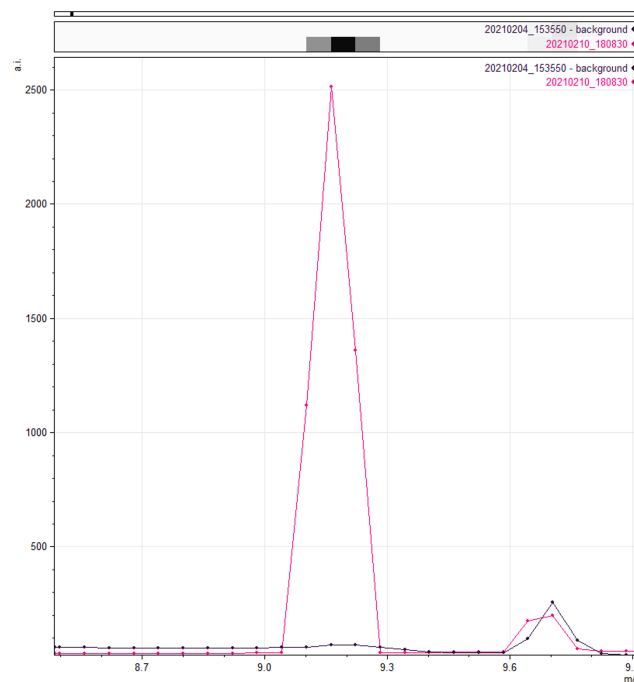


Figure 19: Mass scan data showing a background with no sample (black) compared to a measurement with the sample (pink)

Preliminary efficiency measurements suggest that Be extraction as the molecule  $\text{BeF}_2$  enhances beryllium release both as the molecular beam and as the atomic beam likely resulting from in-source molecular breakup as seen in Figure 19. These protocols will be applied to forthcoming studies, such as the pre-irradiated targets campaign, which aims to start investigations for the LISA program and developments for actinide beams and actinide molecules at ISOLDE, just before protons are back at ISOLDE. Offline developments towards molecular beam development include molecular formation studies at the Offline 1 and Offline 2 mass separators. In collaboration with the MIRACLS team, the MIRACLS Proof-of-Principle (PoP) is another avenue for molecular beam development. At the PoP setup, an ion source is coupled to a Paul trap for bunching and cooling before injection into an offline MR-ToF, offering opportunities for molecular identification.

## References

- [1] M. Götz, S. Götz, J.-V. Kratz, J. Ballof, *Radiochimica Acta* (2021).
- [2] C. Mihai, *et al.*, *Nuclear Instruments and Methods in Physics Research Section A: Accelerators, Spectrometers, Detectors and Associated Equipment* **953**, 163263 (2020).
- [3] V. N. Fedosseev, *et al.*, *Journal of Physics G: Nuclear and Particle Physics* **44**(8), 084006 (2017).
- [4] R. Rossel, *A Distributed Monitoring and Control System for the Laser Ion Source RILIS at CERN-ISOLDE*, Ph.D. thesis, Fachhochschule Wiesbaden (2015).
- [5] V. Samothrakis, *et al.*, 'Isolde newsletter 2020' (2020).
- [6] K. Chrysalidis, *et al.*, *Optics Letters* **44**(16), 3924 (2019).
- [7] D. Echarri, *et al.*, *Optics Express* **28**(6), 8589 (2020).
- [8] R. Bark, C. Fransen, 'Development of  $^{160,162,164}\text{Yb}$  beams: Coulomb Excitation of Triaxial Superdeformed "beta-bands" in light Yb isotopes', Tech. Rep. CERN-INTC-2021-014. INTC-I-226, CERN, Geneva (2021).
- [9] G. Andrea, R. Lica, R. Heinke, A. Andreyev, 'Development of neutron-rich TI beams for nuclear structure studies beyond  $^{208}\text{Pb}$ ', Tech. Rep. CERN-INTC-2020-045. INTC-I-219, CERN, Geneva (2020).
- [10] A. Andreyev, A. Barzakh, T. E. Cocolios, B. Marsh, R. Lica, 'IS456 - Study of polonium isotopes ground-state properties by simultaneous atomic and nuclear spectroscopy', Tech. Rep. CERN-INTC-2019-032. INTC-SR-089, CERN, Geneva (2019).
- [11] R. Heinke, 'Investigation of octupole deformation in neutron-rich actinium using high-resolution in-source laser spectroscopy', Tech. Rep. CERN-INTC-2020-029. INTC-P-556, CERN, Geneva (2020).
- [12] D. Fink, *et al.*, *Nuclear Instruments and Methods in Physics Research Section B: Beam Interactions with Materials and Atoms* **344**, 83 (2015).
- [13] S. Raeder, *et al.*, *The Review of scientific instruments* **85**(3), 033309 (2014).
- [14] S. Richter, *Implementierung der Laserionenquellenfalle LIST bei ISOLDE und Validierung der Spezifikationen Effizienz und Selektivität*, Ph.D. thesis, Johannes Gutenberg-Universität Mainz (2015).
- [15] R. Heinke, *et al.*, *Hyperfine Interactions* **238**(1) (2017).
- [16] R. M. Heinke, *In-source high-resolution spectroscopy of holmium radioisotopes - On-line tailored perpendicular laser interaction at ISOLDE's Laser Ion Source and Trap LIST*, Ph.D. thesis, Johannes Gutenberg-Universität Mainz (2019).
- [17] A. Gottberg, *Nuclear Instruments and Methods in Physics Research Section B: Beam Interactions with Materials and Atoms* **376**, 8 (2016).
- [18] J. P. Ramos, *Nuclear Instruments and Methods in Physics Research Section B: Beam Interactions with Materials and Atoms* **463**, 201 (2020).
- [19] 'CMW website' (2019), <http://cmw.web.cern.ch/CMW/>.
- [20] U. Köster, *et al.*, in *European Physical Journal: Special Topics*, vol. 150, pp. 285–291. Springer-Verlag (2007).
- [21] J. Ballof, *et al.*, *The European Physical Journal A* **55**(5), 65. 11 p (2019).
- [22] 'Cern accelerating science' (2021), <https://lisaitn.web.cern.ch/>.
- [23] T. Wright, 'Fission properties probed via measurements of transfer-induced fission with actinide beams in inverse kinematics using the ISOLDE Solenoidal Spectrometer', Tech. Rep. CERN-INTC-2021-009. INTC-I-224, CERN, Geneva (2021).
- [24] C. Duchemin, *et al.*, 'Radionuclide inventory in targets irradiated at ISOLDE before LS2 in view of long half-life actinide collections at

- CERN-MEDICIS', Tech. Rep. EDMS No. 2379738, CERN, Geneva (2018).
- [25] M. Athanasakis, S. Wilkins, G. Neyens, 'Radioactive molecules at ISOLDE', Tech. Rep. CERN-INTC-2021-017. INTC-I-227, CERN, Geneva (2021).
- [26] U. Köster, 'Yields and spectroscopy of radioactive isotopes at LOHENGRIN and ISOLDE. Ausbeuten und Spektroskopie radioaktiver Isotope bei LOHENGRIN und ISOLDE' (1999), Ph.D. Thesis : Munich, Tech. U. : 1999.

## New electron gun for REXEBIS

Fredrik Wenander for the CERN EBIS team

REXEBIS is an electron beam ion source (EBIS) used for charge breeding of radioactive ions, i.e. transformation from 1+ to a higher charge state of choice, before acceleration in the REX/HIE linear accelerator. During LS2 the electron gun has been upgraded from a conventional magneto-immersed type to a gun using a non-adiabatic magnetic element [1], with the cathode positioned in a low residual magnetic field of 700 Gauss. By doing so, an increased electron current density in the high B-field ion trapping region can be obtained from the magnetic beam compression. As the breeding time is inversely proportional to the current density, this leads to shortened hold-up times in REXTRAP and REXEBIS, and thereby reduced decay losses for short-lived isotopes. Furthermore, the post-accelerator can then be operated with a higher repetition rate, in particular for high-Z elements, and thereby distribute the charge-bred particles over more pulses. A second reason for moving to a new electron gun type was the reliability issues experienced with the previously used  $\text{LaB}_6$  cathodes. After some time of operation, the  $\text{LaB}_6$  crystals developed cracks near the emission head, leading to fluctuating emission current, and in the worst case, detached from the crystal holder.

The new electron gun design was adapted to the existing tight space constraints of REXEBIS. A cross-section showing the actual electron gun with the main elements indicated is presented in Fig. 1. Apart from a new cathode type, now IrCe with a larger diameter of 2 mm, the main feature is the soft iron ring placed after the anode. The ring creates a magnetic field depression of the main guiding field, and when placed in the region of the descending phase of a beam oscillation, the cyclotron motion is reduced and a ripple-free, laminar beam can be generated. Consequently, electron

reflection when entering the field of the main solenoid can be avoided even for a high-emission gun positioned in a magnetic field of only a few hundred Gauss.

The electron gun was extensively tested during the autumn. Even though the nominal electron current has not yet been reached due to limited electron emission from the cathode, numerous results were collected. We could demonstrate that the electron beam exhibits a similar ion injection efficiency as the old gun, in spite of a smaller electron beam radius in full-field region. The breeding time has been cut by a factor 2 to 3. Thus, to reach a charge state distribution that peaks at  $A/Q \sim 4.3$  it now takes approximately 60 ms for  $^{152}\text{Sm}$  and 160 ms for  $^{205}\text{Tl}$ , two of the autumn test beams. Furthermore, residual mass scans showed only very low presence of Ir and Ce ions in the extracted beam. When the operational schedule allows, we plan to test yet another cathode type in order to try to reach the nominal operational current for the gun of 500-700 mA.

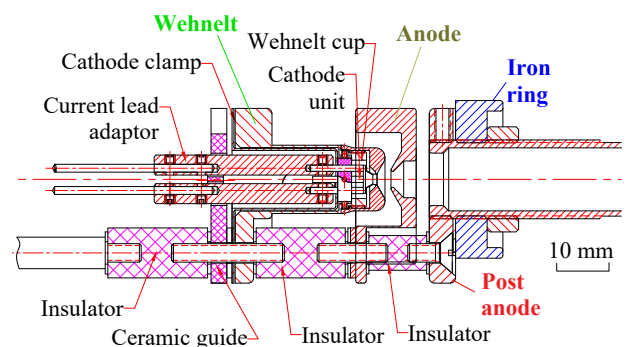


Figure 1: Cross-section of the new REXEBIS electron gun using a non-adiabatic magnetic element for mitigation of electron beam ripples.

## References

- [1] A. Pikin, H. Pahl, F. Wenander, *Physical Review Accelerators and Beams* **23**(10), 103502 (2020).

# RIB Applications

## ASPIC and ASCII: studying 2D materials using radioactive probe atoms

*Koen van Stiphout, Leonard-Alexander Lieske and Hans Hofsäss*

After years of anticipation, the **Apparatus for Surface Physics and Interfaces at CERN (ASPIC)** will make a comeback to the forefront of materials science at ISOLDE [1]! During the 1990's, the experimental setup saw many successful *perturbed angular correlation* (PAC) experiments, leading to a number of publications on the magnetic properties of single crystal and thin film surfaces and interfaces [2]. Since that time, however, ASPIC has not been active anymore, due to a lack of financial support and dedicated manpower. Soon, it will make a comeback, turning its attention to low-energy PAC isotope implantation ( $^{111m}\text{Cd}$ ,  $^{77}\text{Se}$ ,  $^{204m}\text{Pb}$ ,  $^{68m}\text{Cu}$ ...) into nanostructures at the cutting edge of solid state physics, such as 2D materials (graphene,  $\text{MoS}_2$ ...), (multi)ferroic materials and topological insulators.

The setup is currently being upgraded at the university of Göttingen, after which it will be moved back to the ISOLDE experimental hall. As before, ASPIC will offer a variety of surface and thin film modification techniques (deposition, ion sputtering, annealing) and characterization methods (Auger electron spectroscopy, low-energy electron diffraction (LEED)), allowing the preparation of clean surfaces without breaking the ultra-high vacuum ( $\leq 10^{-9}$  mbar).

The ASPIC will be complimented by a brand-new chamber: the **Apparatus for Surface physics and interfaces at CERN's Ion Implantation chamber (ASCII)**. In this extension, a custom-made deceleration unit will be installed, which slows the ISOLDE ion beams down from 60 keV to energies on the order of 10 eV (Fig. 1). These PAC ions are focused onto the surface of

the sample, allowing fast incorporation of PAC probes into the studied materials. This new ion beam setup will replace the slower and more cumbersome catcher system that was used in ASPIC before. Faster implantation and quick transfer allow for more samples to be measured during beamtimes, as well as increase the signal-to-noise ratio during PAC measurements. The ASCII, combined with the wide range of thin film configurations that ASPIC offers, will provide users with precise control of the location of PAC probes in nanofilm structures. Commissioning and testing of these chambers will continue throughout 2021. Their return to ISOLDE is planned for late 2021, early 2022.

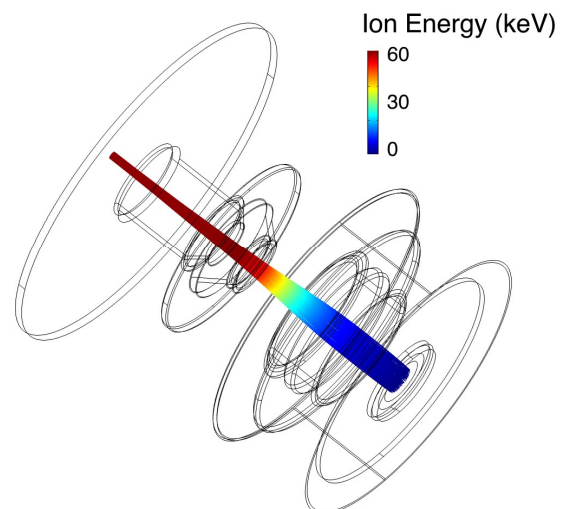


Figure 1: Using the deceleration stage of the ASCII, PAC isotopes will be implanted unto sample surfaces with energies as low as 10 eV.

<https://www.uni-goettingen.de/de/550904.html>

## References

- [1] H. Hofsäss, K. van Stiphout, 'Letter of Intent: Upgrade of the UHV-system ASPIC for the investigation of surfaces and two-dimensional materials by ultra-low energy implantation and deposition of radioactive probe atoms (*CERN-INTC-2020-001; INTC-I-208*)', Tech. rep. (2020).
- [2] H. Bertschat, *et al.*, *Hyperfine Interactions* **129**(1), 475 (2000).

## Quantum colour centers in diamond studied by emission channeling with short-lived isotopes (EC-SLI) and radiotracer photoluminescence

Results and outlook for experiment IS668

Ulrich Wahl for the EC-SLI collaboration

Dopant-vacancy centers represent qubits in diamond with associated free electrons and multiple spin states in superposition. Reliable write-in/read-out of qubit states requires minimal spectral diffusion and dispersion, thus large Debye-Waller factors and narrow inhomogeneous linewidth. Group-IV impurity elements (Si, Ge, Sn, Pb), with larger electronic radii than C, are expected to favour bond center (BC) sites in the so-called “split-vacancy” group-IV-V configuration (Fig. 1) where the molecular  $D_{3d}$  inversion symmetry makes the optical transition frequency particularly insensitive to electric field noise [1].

Our recent application for experiment IS668 (approved at the 64<sup>th</sup> Meeting of the INTC) was motivated by the fact that emission channeling (EC) has been the only experimental method capable of directly detecting and quantifying ion implanted impurities in diamond in the so-called “split-vacancy” configuration, which is supposed to be responsible for the remarkable optical properties of the centers. For that purpose, we combined EC data from the decay of  $^{121}\text{Sn}$  (27 h) with photoluminescence on  $^{121\text{m}}\text{Sn}$  (55 y) implanted into a natural diamond sample, showing the existence of a large fraction of Sn on “double vacancy” BC sites and sharp photoluminescence lines corresponding to  $\text{SnV}^-$  at room temperature (Fig. 1, [2]). The 2.3 nm linewidth of the zero phonon line at 621 nm (with near-perfect Lorentzian shape, i.e. limited by luminescence lifetime) is the narrowest so far reported in the literature for an ensemble of  $\text{SnV}^-$  at RT.

IS668 proposes studying the lattice locations of implanted radioactive isotopes of colour center elements in natural and synthetic diamond single crystals using EC and to correlate this information with the optical properties of the centers as determined by radiotracer photoluminescence (PL). Moreover, in a new approach, we aim at investigating the influence of implantation

temperature and of implantation under channeling conditions in order to critically reduce implantation-induced defects in diamond. The major effort will focus on the  $\text{SnV}^-$  defect, currently one of the most-promising single photon emitters for quantum applications [1]. However, other impurity colour centers that have been described in the literature and that are also envisaged to be addressed include Si, Ge, Pb, Mg, Ca, Sr, and also the noble gases He, Ne, Ar, Kr and Xe, although to a lesser extent than Sn. IS668 attracted new ISOLDE users from the field of quantum defects in diamond and will also imply a major refurbishment of the existing PL lab at ISOLDE.

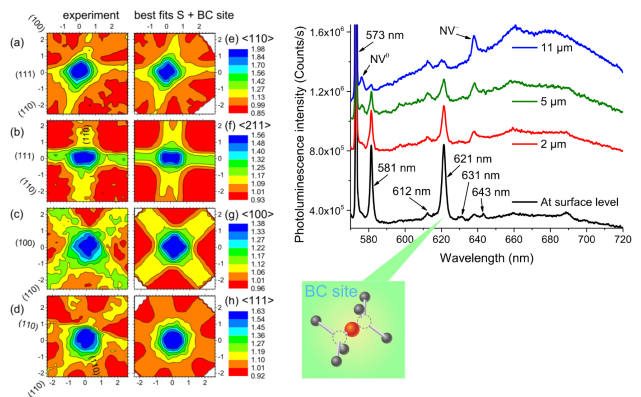


Figure 1: (a)–(d): Experimental  $\beta^-$  EC patterns from  $^{121}\text{Sn}$  implanted diamond following 920°C annealing. (e)–(h): corresponding best fits of theoretical patterns considering 79% on ideal substitutional and 32% on ideal BC sites. Right: confocal PL spectra following the decay of  $^{121}\text{Sn}$  to  $^{121}\text{Sb}$ , i.e.,  $\text{SnV}^-$  related lines, with the major component at 621 nm, result from long-lived  $^{121\text{m}}\text{Sn}$ . The spectra were recorded at room temperature under 532 nm laser excitation with the focus at various depths. Bottom center: The atomic structure of  $\text{SnV}^-$  in the split-vacancy configuration.

## References

- [1] C. Bradac, W. Gao, J. Forneris, M. E. Trusheim, I. Aharonovich, *Nat. Commun.* (10), 5625 (2019).
- [2] U. Wahl, *et al.*, *Phys. Rev. Lett.* (125), 045301 (2020).

# Local probing $\text{Ca}_2\text{MnO}_4$ structural phase diagram and negative thermal expansion properties

Results of experiment IS647

Pedro Rocha-Rodrigues, Armandina Lopes  
for the IS647 collaboration

Within the framework of IS647 "Local Probing of Ferroic And Multiferroic Compounds" a comprehensive study on multiferroic materials is ongoing, including materials in which the ferroelectricity order arises from proper, improper and hybrid improper mechanisms. In this respect, naturally layered perovskites such as the Ruddlesden-Popper (RP) phases, with general formula  $\text{AO}(\text{ABO}_3)_n$  (A: rare earth or alkaline-earth and B: transition metal) are studied as alternative routes to develop and design novel functional materials, ranging from multiferroics, to photovoltaic systems, to materials that display uniaxial negative thermal expansion (NTE) [1, 2]. In these RP layered perovskites the hybrid improper ferroelectricity originates not from a simple cation off-centering but by appropriate octahedral tilt combinations that result in a polar symmetry. Furthermore, the NTE, arises also from a combination of the RP layered structure with the condensation of a particular set of  $\text{BO}_6$  octahedral distortion modes [2]. An atomic corkscrew mechanism was recently proposed, treating  $\text{BO}_6$  octahedra as rigid units, where the stiff nature of A-O bonds play a crucial role in coupling the decrease of  $\text{BO}_6$  octahedra rotation distortion to the lattice contraction along the layering-axis [3]. As this mechanism operates at the interfaces between the AO and  $(\text{ABO}_3)_n$  layers, the lower dimensional element  $\text{Ca}_2\text{MnO}_4$  ( $n=1$ ) is expected to have the highest uniaxial NTE of its RP series. Nevertheless, experimentally, long range order based techniques such as x-ray or neutron diffraction are known to present difficulties in correlating, with precision, the evolution of octahedral rotations with the thermal change of the  $\text{Ca}_2\text{MnO}_4$  expansion properties, either due to a lower sensitivity to oxygen atomic positions, as in x-ray diffraction, or due to low structural coherence lengths within the  $\text{Ca}_2\text{MnO}_4$

crystal lattice, that attenuate the intensity of the Bragg reflections sensitive to the  $\text{MnO}_6$  octahedra rotation pattern.

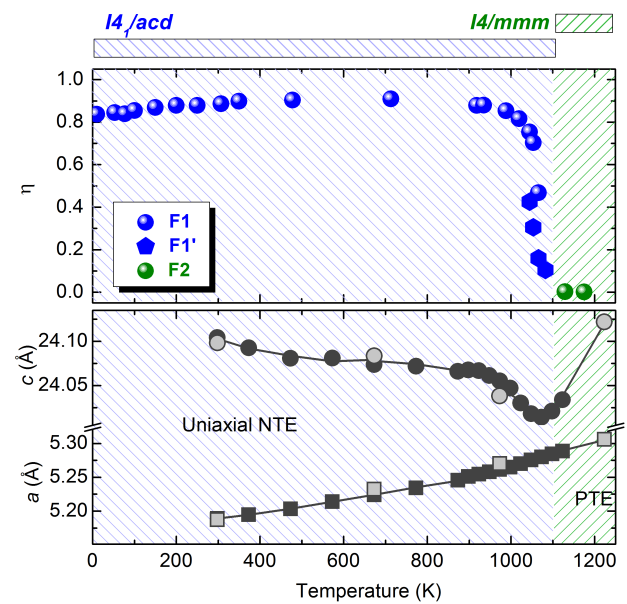


Figure 1: Experimental electric field gradient asymmetry parameter,  $\eta$ , and  $\text{Ca}_2\text{MnO}_4$   $a$  and  $c$  lattice parameters, highlighting the increase of axial symmetry from the distorted  $I4_1/acd$  structure to the arystotype  $I4/mmm$  phase and the concomitant enhancement of the uniaxial NTE close to the structural transition. For the  $I4/mmm$  phase,  $\sqrt{2}a$  and  $2c$  values are plotted.

Time differential perturbed angular correlation (TD-PAC) experiments combined with neutron and x-ray diffraction measurements, and density functional theory simulations provide a unique tool to characterize the  $\text{Ca}_2\text{MnO}_4$  structural transitions at the atomic scale [1]. The detailed measurement of the electric field gradient (EFG), and local symmetry analysis, allow an accurate probe of the  $\text{MnO}_6$  octahedral rotations which underlie the  $\text{Ca}_2\text{MnO}_4$  structural transitions and the uniaxial NTE properties. TDPAC measurements were performed at ISOLDE for a wide temperature range (11-1200 K) using  $^{111m}\text{Cd}$ . [2] Our studies confirmed that the phase that stabilises at the high temperatures has

the arystotype  $I4/mmm$  symmetry, establishing also the critical temperature for the  $I4_1/acd$  to the  $I4/mmm$  second order phase transition to be around 1050 K, at much lower temperature than previously predicted. Direct evidence for the corkscrew atomic mechanism governing the enhancement of the uniaxial NTE close to the critical temperature was obtained, as shown in Fig. 1, highlighting the increase of axial symmetry from the distorted  $I4_1/acd$  structure to the arystotype  $I4/mmm$  phase (decrease in  $\text{BO}_6$  octahedra rotation) and the enhancement of the lattice contraction along the layering  $c$ -axis. Moreover, at room temperature a single local environment was found, in order to explain the lower coherence length observed along the

layering-axis in previous measurements, we have clarified that the previously reported  $Aba2$  structural phase of the  $\text{Ca}_2\text{MnO}_4$  should be described instead in the higher symmetry  $Acam$  space group [2].

## References

- [1] P. Rocha-Rodrigues, *et al.*, *Physical Review B* **101**(6), 064103 (2020).
- [2] P. Rocha-Rodrigues, *et al.*, *Physical Review B* **102**(10), 1 (2020).
- [3] C. Ablitt, A. A. Mostofi, N. C. Bristowe, M. S. Senn, *Frontiers in Chemistry* **6**(10), 1 (2018).

## Preparing xenon samples for future medical applications of $\gamma$ MRI

Results of LOI I-205  
on production of Xe isomers

*Karolina Kulesz and Magdalena Kowalska  
for the gamma-MRI collaboration*

Xenon isotopes have become very useful in Single Photon Emission Computed Tomography (SPECT) and Magnetic Resonance Imaging (MRI) medical diagnosis ( $^{133}\text{Xe}$  with 5-day half-life and stable  $^{129}\text{Xe}$ , respectively). Well-documented clinical use, existing spin-polarization techniques, and medically suitable half-lives also make several other xenon isotopes great candidates for the development of novel imaging modalities.

The goal of letter of intent I-205 was to produce xenon isomers  $^{129m,131m,133m}\text{Xe}$ , polarize their spins using Spin Exchange Optical Pumping (SEOP), and detect asymmetry in their gamma emission. These are the first steps towards a new medical modality devoted to radiation-detected MRI [1]. For this purpose, several setups were assembled, including one to trap Xe and transfer it into a polarization cell, and most notably another for detection of polarization, which combines elements of a convectional SEOP device with gamma detectors.

In 2018, we tested the feasibility of  $^{131m,133m}\text{Xe}$  production at ISOLDE, using  $\text{ThC}_x$  and  $\text{UC}_x$  targets coupled to a cooled plasma source. Isotopes with mass/charge ratio equal to 133 were transported through the GPS magnet and collected on thin foils at the GLM beamline. Different implantation materials were tested, including tantalum, carbon and aluminum (see Fig. 1, right) to optimize subsequent xenon extraction. The production of  $^{131m}\text{Xe}$  was also investigated with both targets, but no  $^{131m}\text{Xe}$  gamma activity was visible in the intense background at mass 131. This observation is not yet understood and further tests within INTC-P-598 [2] are required to investigate it. In-situ gamma-spectroscopy of the foils allowed the  $^{133m}\text{Xe}$  released from the target to be estimated. The activity collected at each of the foils was in the range of 80

to 280 MBq.

During LS2, we worked on Xe production via neutron activation at ILL in Grenoble. For this purpose, stable isotopes of  $^{128}\text{Xe}$  and  $^{130}\text{Xe}$  were enclosed in quartz ampoules (Fig. 1) and placed in the shaft of the nuclear reactor at ILL, in the beam of thermal neutrons (25 meV; 2.2 km/s) with a flux of  $10^{15}$  n/s·cm<sup>2</sup>. After a 7-day-long irradiation, the ampoules were shipped back to CERN and their content, then including  $^{129m}\text{Xe}$  and  $^{131m}\text{Xe}$ , was transferred into a vial immersed in a LN<sub>2</sub> cold trap. Gamma spectroscopy performed on the samples before and after the transfer indicated that the efficiency of xenon transfer was 70%, with 120 to 200 MBq in the final vial.



Figure 1: Left: Enclosed stable Xe sample ready for neutron capture at ILL. Right: metal matrix used for Xe implantation at the GLM beamline.

The setup for polarization and gamma acquisition, once assembled and tested, was installed temporarily in building 508. The system (Fig. 2) was composed of an infra-red laser system for optical pumping of rubidium atoms, the static magnetic field necessary for the choice of the nuclear orientation axis, and a heating system providing thermal optimum for the SEOP process.

Instead of RF detection coils, the experimental setup was equipped with fast gamma detectors, namely three GAGG(Ce) detectors (referred to as detector 1, 2 and 3 in Fig. 1) and one LaBr(Ce) detector (detector 4 in Fig. 1), coupled to SiPMs that are not influenced by the magnetic field.

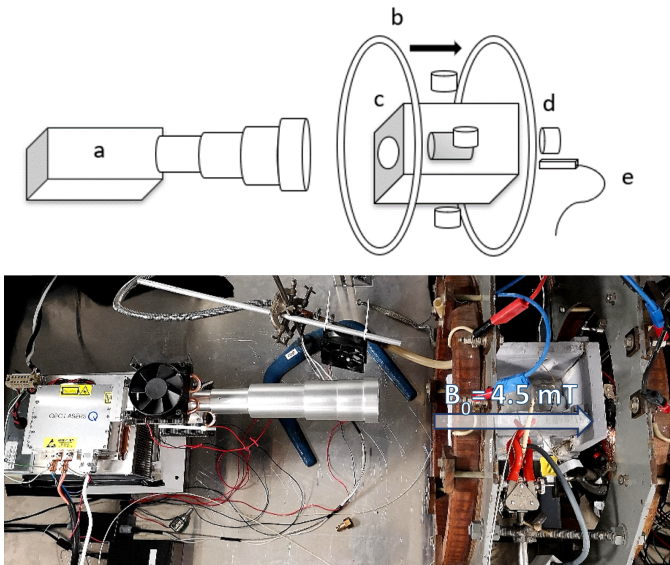


Figure 2: A scheme (top) and a photo (bottom) of the polarizer with detectors: (a) laser diode array with the telescopic lenses; (b) a pair of Helmholtz coils; (c) an insulating oven accommodating the pumping cell; gamma detectors: three GAGG:Ce crystals (d) and one LaBr3:Ce crystal (e) coupled to SiPMs.

The aim of the experiments was to prove the creation of Xe spin alignment and its further optimisation. The alignment was observed via gamma asymmetry between detectors placed at 0 and 90 degrees to the direction of the magnetic field. Following a series of measurements and a systematic data analysis (see the calibrated spectrum in Fig. 1), the experimental asymmetry of  $^{129m}\text{Xe}$  gamma emission was estimated at the level of 1 to 2% for pairs of detectors situated in orthogonal planes. Simulations focused on linking this level of asymmetry to the value of nuclear alignment and polarization are ongoing.

The initiative to create a novel biomedical imaging modality resulted in a recently established official collaboration between our group at CERN with the University of Applied Sciences and Arts of Western Switzerland (HES-SO), the University of Geneva, Complutense University of Madrid (UCM), RS2D, and KU Leuven and

Tecnologias Avanzadas Inspiralia SL.

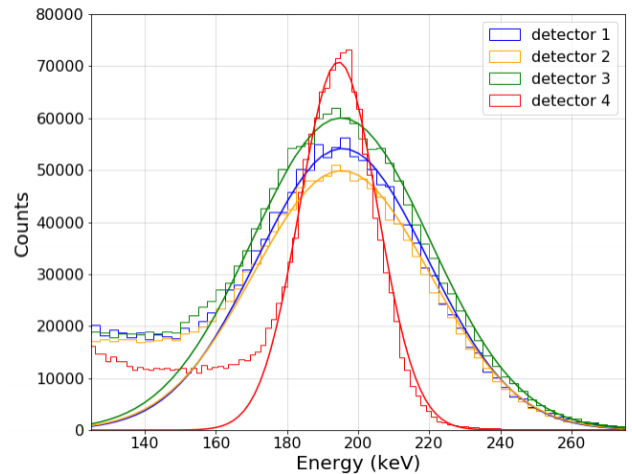


Figure 3: Calibrated spectra of  $^{129m}\text{Xe}$  decay registered with the four detectors. Single Gaussian fitting was applied and the area under the fits was used to determine the gamma asymmetry value.

A European Union Horizon2020 funding for “Novel ideas for radically new technologies” (FET Open 2021-2024, project GAMMA-MRI n. 964644) has assured continuation and expansion of the gamma-MRI project for at least 3 years with the aim to build and test a pre-clinical prototype of a gamma-MRI setup. ISOLDE’s contribution includes the research of the most cost effective production routes of mXe isotopes and the high purification of the samples before any further in vivo or in vitro manipulation.

References

[1] Y. Zheng, G. W. Miller, W. A. Tobias, G. D. Cates, *Nature* **537**(7622), 652 (2016).  
 [2] K. Kulesz, M. Kowalska, ‘Collection of  $^{129m},^{131m},^{133m}\text{Xe}$  for the gamma-MRI project’, Tech. Rep. CERN-INTC-2021-019. INTC-P-598, CERN, Geneva (2021).

# Ground-state properties

## High-resolution Laser Spectroscopy of $^{27-32}\text{Al}$

Results of experiment IS617

Charlie Devlin for the COLLAPS collaboration

Laser spectroscopy provides model-independent access to the electromagnetic moments and changes in the mean-square charge radius of nuclei; such measurements are therefore ideal candidates to test nuclear theories. As well as a test of the quality of theoretical calculations in a mid-shell region, the aluminum chain ( $Z = 13$ ) allows us to probe nuclear effects as we approach the  $N = 20$  shell closure.

In experiment IS617, the hyperfine spectra of  $^{27-32}\text{Al}$  were measured on the  $3s^23p\ ^2P_{3/2}^0 \rightarrow 3s^24s\ ^2S_{1/2}$  atomic transition at  $25235.696\text{ cm}^{-1}$ . The ion beam was cooled and bunched with ISCOOL before being guided through the COLLAPS beamline where a Doppler-tuning voltage was applied to each bunch before it was passed through a charge exchange cell and overlapped with  $\approx 2\text{ mW}$  of continuous-wave laser light. The resulting fluorescence photons were detected by photomultiplier tubes and signals were gated offline such that only those which coincide with the passage of a bunch through the interaction region are counted towards the spectrum.

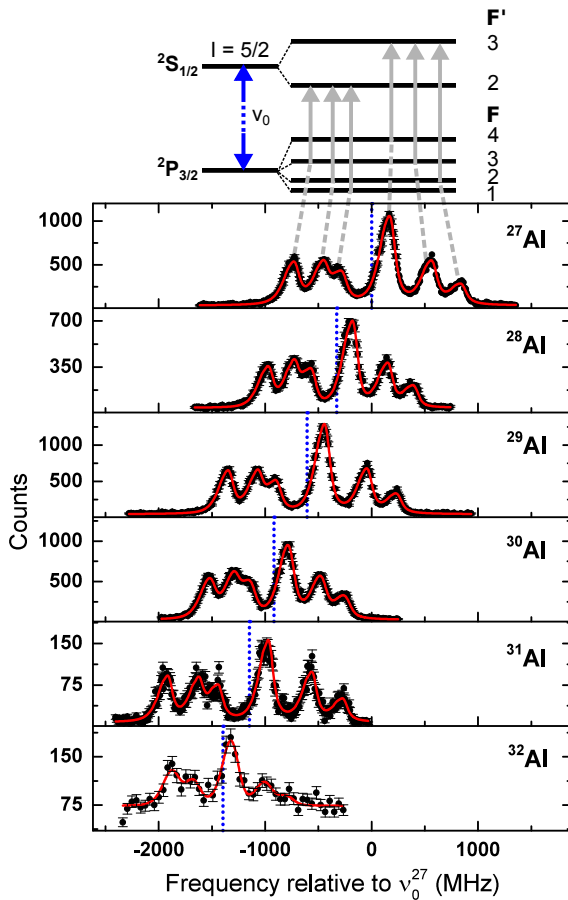


Figure 1: The hyperfine structure of  $^{27-31}\text{Al}$  as measured on the  $3s^23p\ ^2P_{3/2}^0 \rightarrow 3s^24s\ ^2S_{1/2}$  atomic transition. The dashed blue line in each spectrum represents its centroid, while an example of the hyperfine energy levels in  $^{27}\text{Al}$  is shown at the top of the figure [1].

<https://collaps.web.cern.ch>

The magnetic dipole and electric quadrupole moments were extracted, yielding measurements of the magnetic moment of  $^{29}\text{Al}$  and the quadrupole moments of  $^{29,30}\text{Al}$  for the first time [1]. Furthermore, the newly measured changes in the mean-square charge radius show a possible reduction at  $N = 19$ , potentially demonstrating signs of a shell closure effect at  $N = 20$ . However, the measurement at  $N = 19$  is subject to large uncertainties and such an effect has not been seen in neighbouring chains. Hence, a more precise measurement of this isotope is suggested to clarify this issue.

The nuclear properties for the Al isotopic chain were calculated by the VS-IMSRG method [2]. It was seen that the trend in nuclear magnetic and quadrupole moments were well reproduced across the chain while the mean-square charge radii proved to be more difficult, both for the absolute scale and the trend. This finding is in contrast with recent results from other odd- $Z$  isotopic chains where theoretical calculations followed

the experimental trend [3, 4]. This highlights the importance of a variety of observables and experimental input from many isotopic chains to better understand the capabilities of state-of-the-art nuclear theories. Moving forwards, a high-resolution measurement of the isomeric shift between the ground state of  $^{26}\text{Al}$  and its isomer would provide an ideal probe of the proton-neutron pairing correlations in a self-conjugate nucleus.

## References

- [1] H. Heylen, *et al.*, *Phys. Rev. C* **103**, 014318 (2021).
- [2] K. Tsukiyama, S. K. Bogner, A. Schwenk, *Phys. Rev. C* **85**, 061304 (2012).
- [3] R. de Groote, *et al.*, *Nature Physics* **16**, 620 (2020).
- [4] J. Simonis, S. R. Stroberg, K. Hebeler, J. D. Holt, A. Schwenk, *Physical Review C* **96**, 014303 (2017).

## A year of success at CRIS

Results of experiments IS531, IS620, IS657

Michail Athanasakis-Kaklamanakis, Holly A. Perrett  
for the CRIS collaboration

During the Long Shutdown 2 at CERN, the collinear resonance ionization spectroscopy (CRIS) experiment saw a successful year with among others, three publications in *Nature* journals: the first laser spectroscopy on short-lived radioactive RaF molecules [1], challenging the magicity of the  $N = 32$  neutron number in K isotopes [2], and shedding light on the nature of the odd-even staggering (OES) in exotic Cu isotopes [3].

The successful RaF run in 2018 led to the CRIS collaboration's first publication in *Nature* in May 2020 [1], describing the experimental method used to produce the short-lived radioactive molecules and determine their low-lying vibronic structure. A two-step laser scheme was employed for measuring the energies of these electronic and vibrational transitions. This publication represents a milestone in demonstrating the versatility of the CRIS technique, opening up the possibility of studying other radioactive molecules, including those containing nuclei with lifetimes as short as a few tens of milliseconds.

RaF molecules have been shown to be particularly sensitive to parity- and time-reversal-violating effects that could be measured in trap experiments utilizing laser-cooling techniques, while certain strong nuclear-spin-dependent parity-violating effects could potentially be within reach for in-flight experiments. As a requirement for laser cooling, the molecules under study must have closed transitions that can be continually excited and de-excited, with the upper state having a sufficiently short lifetime such that the process can be performed rapidly. The results presented in Ref. [1] (Fig. 1) indicate that RaF molecules would indeed be a suitable candidate for studies involving direct laser cooling.

In addition, ongoing analysis of data from the RaF run yielded a measurement of the ionization threshold of  $^{226}\text{Ra}^{19}\text{F}$ , which was found to be in excellent

agreement with the value predicted by *ab initio* quantum chemistry calculations. Starting from the vicinity of

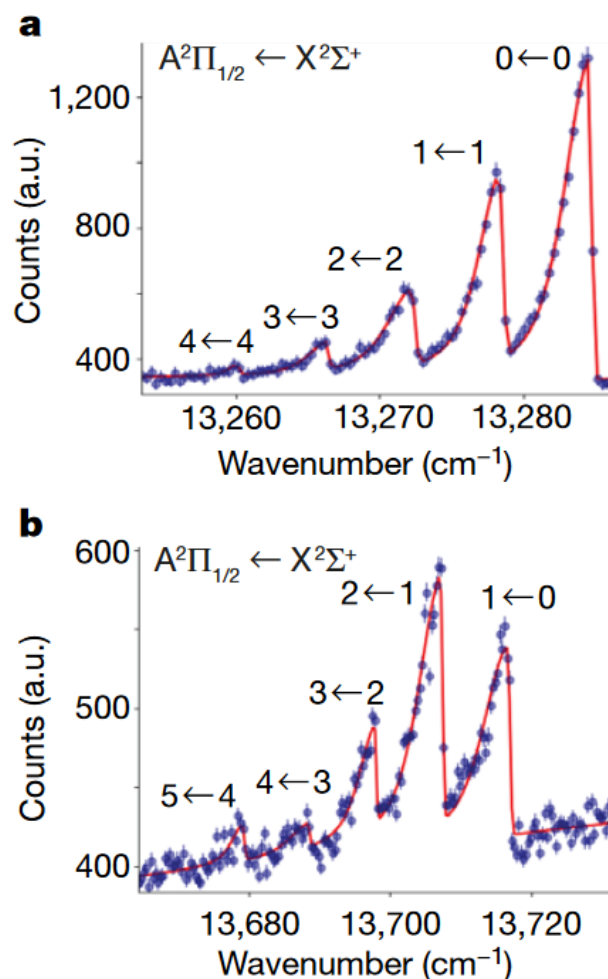


Figure 1: Examples of vibronic spectra measured for  $^{226}\text{RaF}$ . Peaks correspond to electronic transitions with a lower ( $\nu'$ ) and an upper ( $\nu''$ ) vibrational state. In **a**,  $\nu' = \nu''$ , while in **b**,  $\nu' = \nu'' - 1$ . Appears as Fig. 2 in Ref. [1].

the *ab initio* prediction, the  $\text{RaF}^+$  count rate was measured for a series of ionization laser frequencies. This made it possible to determine the threshold frequency at which an enhancement of the ion count rate was observed.

This measurement constitutes an important benchmark for quantum chemistry calculations, paving the way for predicting the properties of more complex ra-

dioactive molecules. It also furthers understanding of the diatomic bonding in Group II monohalides and the behavior of the characteristic non-bonding electron, thus serving as a tool for studying the relative impacts of atomic and molecular effects on electronic structure and chemical bonding.

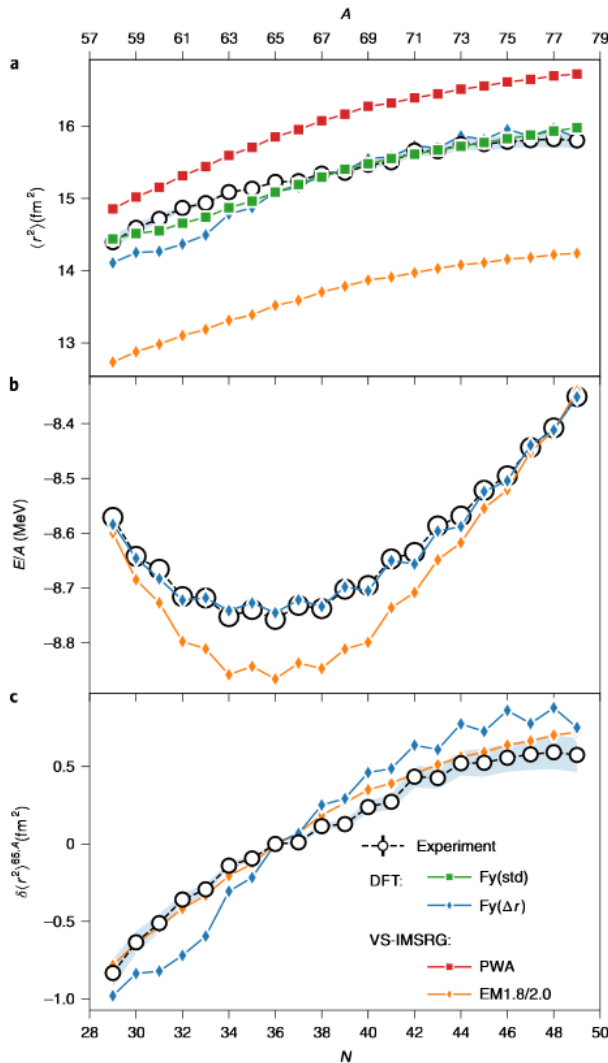


Figure 2: Comparison of selected experimental data and nuclear theory predictions of the nuclear structure of Cu isotopes, up to the highly unstable  $^{78}\text{Cu}$ . Appears as Fig. 2 in Ref. [3].

The high resolution and sensitivity of the CRIS experiment was also used to report new measurements of the mean-squared charge radii of the neutron-rich Cu isotopes up to  $^{78}\text{Cu}_{49}$ , which was produced at a rate of  $\sim 20$  ions  $\text{s}^{-1}$ , shedding light upon the evolution of the OES in the vicinity of  $N = 50$ .

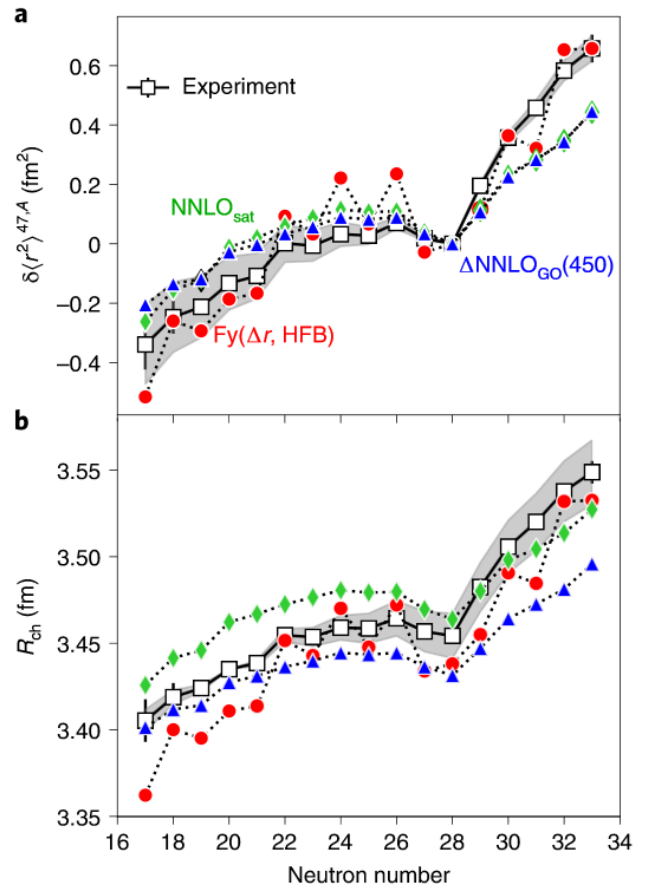


Figure 3: Comparison of experimental charge radii and theoretical predictions for neutron-rich K isotopes. Appears as Fig. 3 in Ref. [2].

de Groote et al. [3] compared the mean-squared charge radii, the binding energies per nucleon, the differential charge radii with respect to  $^{65}\text{Cu}$ , as well as the three-point staggering parameters of the binding energies and the radii against theoretical predictions. Despite the inherent complexity of odd- $Z$  nuclei in the medium-mass region, the theoretical predictions made with two density functional theory (DFT) parametrizations, the Fy(std) and the Fy( $\Delta r$ ) Fayans functionals, and with the valence-space in-medium similarity renormalization group (VS-IMSRG) based on the PWA and the EM1.8/2.0 interactions, proved to be in good agreement with the experimental measurements (Fig. 2). Such agreement is a major achievement for nuclear theory. DFT, which in general is better at capturing bulk nuclear properties, is more successful in reproducing the total charge radii and binding energies, while VS-IMSRG, better at capturing local variations, shows success in reproducing the OES in these observables. The

success of each method in reproducing the different observables provides insight into the microscopic nature of the evolutionary trends of these properties along the isotopic chain.

Contrary to the triumph of nuclear theory in the case of neutron-rich Cu isotopes, the charge radii of neutron-rich K isotopes, present a challenge to both theory and previous experiments on these observables that have so far supported that the  $N = 32$  neutron number is magic [2].

Nuclei around the calcium region that contain 32 neutrons have previously been observed to have increased stability compared to their neighbors, evident through a sudden decrease in the binding energy if neutrons are added beyond  $N = 32$ . Such behavior, which suggests that  $N = 32$  is a magic neutron number, would be expected to cause a sudden increase in the mean-squared charge radius of  $^{52}\text{K}$ , which has one neutron more than this magic number. Koszorús et al. measured the differential mean-squared charged radii of neutron-rich K isotopes with respect to that of the reference isotope  $^{39}\text{K}$ , and observed no such change of trend immediately after  $N = 32$ .

To test the ability of state-of-the-art nuclear theory to reproduce the observed trends in differential and absolute charge radii on neutron-rich K isotopes, Koszorús et al. compared the experimental measurements with DFT and coupled-cluster (CC) calculations based on the  $\text{Fy}(\Delta r, \text{HFB})$  optimization and the  $\text{NNLO}_{\text{sat}}$

and  $\Delta\text{NNLO}_{\text{GO}}(450)$  interactions, respectively (Fig. 3). While the DFT framework reproduced the global increase in radii in the neutron-rich side sufficiently well, it overestimates the OES along the chain. Inversely, while the CC calculations do not overestimate the OES, they fail to predict the steep increase in radii beyond  $N = 28$ . The unsatisfactory reproduction of these observations by modern nuclear theory highlights our current lack of sufficient understanding about these nuclear systems, and provides motivation for the continued improvement of our nuclear models.

In summary, 2020 was a successful year for the CRIS collaboration. With landmark technical and scientific achievements in nuclear and molecular physics, the collaboration provided important contributions to the potential use of radioactive molecules in fundamental physics and chemistry, performed laser spectroscopy on very unstable isotopes for the first time with remarkable sensitivity and resolution, and challenged state-of-the-art nuclear models, while validating the accuracy of others.

## References

- [1] R. F. Garcia Ruiz, *et al.*, *Nature* **581**(5), 396 (2020).
- [2] Á. Koszorús, *et al.*, *Nature Physics* **17**, 439 (2021).
- [3] R. P. de Groote, *et al.*, *Nature Physics* **16**(6), 620 (2020).

## A New Laser Ablation Source For ISOLTRAP

Lukas Nies for the ISOLTRAP collaboration

The ISOLTRAP mass spectrometer at ISOLDE/CERN has a long history of developing and operating laser ablation ion sources (LAS) for the use in low-energy precision mass spectrometry, dating back almost 20 years [1].

Laser-ablated carbon clusters can be used as reference ions for absolute mass measurements and are covering the nuclear chart (see Fig. 1a). Additionally, reference ions from a wide mass range are useful for extensive systematic studies of mass-dependent uncertainties of the different mass measurement techniques available at ISOLTRAP, as demonstrated for the time-of-flight ion-cyclotron-resonance (ToF-ICR) technique [2]. Furthermore, laser-ablated ions from long-lived radioactive or stable targets provide a source for precision Q-value measurements [3].

Due to a remodeling of ISOLTRAP's vertical beam-line and the installation of a multi-reflection time-of-flight device it became necessary to relocate the old LAS installation to a new position. The new setup will be at the location of the alkali offline source with the new design intended to incorporate both sources. This new location has several advantages: being positioned upstream of all ion trap systems, the reference ions will undergo the same flight path as the online beam and can be used for characterization and reference in all traps. A picture of the current state of assembly can be found in Fig. 1b.

Figure 1c shows a CAD drawing of the new source setup. Due to space-constraints and the necessity of being located on a high-voltage platform, the ablation laser is placed on top of a Faraday cage. The laser beam is guided down with several optical elements into the ablation target chamber. Using a quadrupole bender, the new source setup can deliver either laser-ablated ions or surface-ionized ions. The assembly is

in progress and will be ready by late Spring for commissioning and testing before the start of the ISOLDE physics program.

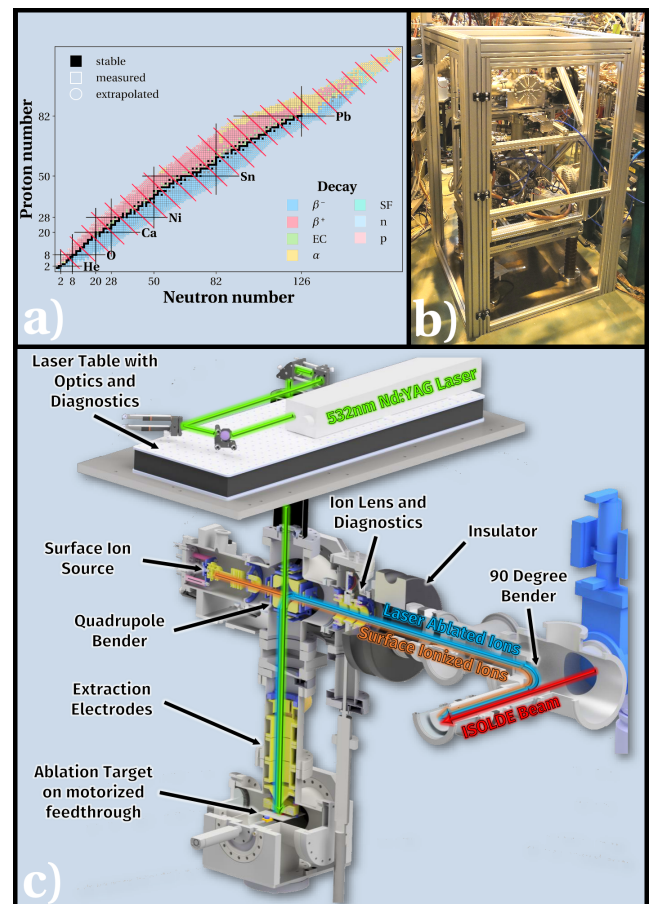


Figure 1: a) Possible reference masses with carbon clusters across the nuclide chart highlighted with red stripes. b) Current state of assembly. The source is located on a 60 kV high-voltage platform inside a Faraday cage. c) CAD drawing for the new offline source setup at ISOLTRAP, incorporating a surface ionization source (alkali ions) and the LAS.

## References

- [1] K. Blaum, *Eur. Phys. J. A* **15**(245–248) (2002).
- [2] A. Kellerbauer, *Eur. Phys. J. D* **22**(1), 53 (2003).
- [3] D. Fink, *Phys. Rev. Lett.* **108**(6) (2012).

## Nuclear structure of $^{181}\text{Au}$

Results of experiment IS521

Matúš Sedlák and Martin Venhart  
for the IS521 collaboration

The experiment [1] proposed to study of odd-mass Au isotopes was carried out in 2014 and 2016 at the LA1 beamline of the ISOLDE facility, where the TATRA spectrometer [2] was employed. TATRA uses metallic tape prepared by rapid quenching of an alloy for transportation of radioactive samples from the irradiation point to its detector station, where two standard coaxial germanium detectors and a single Broad Energy Germanium detector are located. The data were acquired with a fully-digital acquisition system, based on the commercial Pixie-16 14 bit, 250 MHz digitisers.

A method [3] based on the time structured data was used for data analysis of  $^{181}\text{Hg}$  decay to  $^{181}\text{Au}$ , which was also successfully used in the  $^{183}\text{Hg}$  decay study [4]. This method is described in Fig. 1 together with a result of the fitting procedure of the BEGe singles spectrum. The partial decay scheme from  $^{181}\text{Hg} \rightarrow ^{181}\text{Au}$  was constructed for the first time [1]. The proposed level scheme was constructed on the basis of the Rydberg-Ritz analysis and coincidence relationships. The first excited state was established with the energy of 1.79 keV. The previous study of the  $^{181}\text{Hg}$  decay [5] reported no level scheme and a list of 20 transitions, but only 8 of them were confirmed by the present experiment. Most notably, the study [5] does not report the strongest 111.34 and 113.11 keV transitions.

Excited states associated with the  $1h_{11/2}$  proton-hole configuration were identified and the systematics of these states in odd-Au isotopes were extended. Slightly increasing excitation energies of  $7/2^-$  and  $3/2^-$  states with decreasing neutron number could indicate, based on the particle-plus-triaxial-rotor model (PTRM) [6, 7], a slow transition from weakly oblate-deformed to prolate shape in light Hg isotopes.

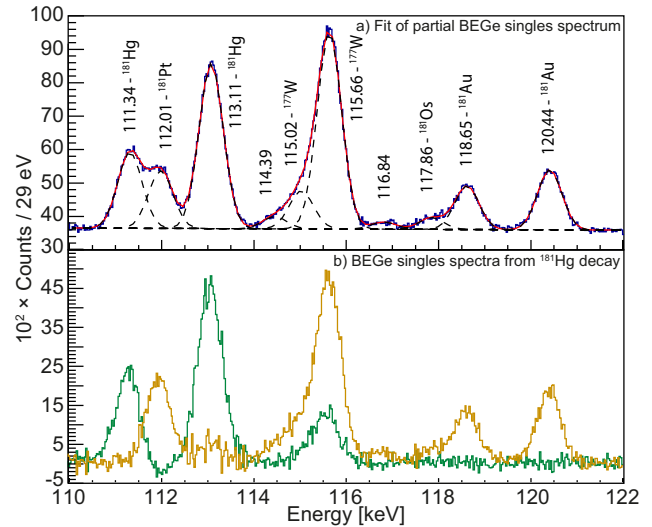


Figure 1: **a)** Part of the  $\gamma$ -ray singles spectrum detected with the BE2020 BEGe detector (blue line), a fit (red line) with multiple Gaussian peaks (black dashed line) and with linear background. A reduced  $\chi^2$  for the fit is of 1.03. **b)** Part of the deconvoluted singles spectra measured with the BE2020 BEGe detector [3]. The spectrum assigned to  $^{181}\text{Hg}$  decay is depicted by a green colour while the spectrum assigned to daughter decays is depicted by an orange line. Parameters of the deconvolution were tuned to subtract transitions of the  $^{181}\text{Au}$  decay (dominant contamination) and therefore the 115.66 keV peak from the  $^{177}\text{W}$  decay remains in the spectrum. See [1] for more details.

## References

- [1] M. Sedlák, *et al.*, *Eur. Phys. J. A* **56**, 161 (2020).
- [2] V. Matoušek, *et al.*, *Nucl. Instrum. Meth. A* **812**, 118 (2016).
- [3] M. Venhart, *et al.*, *Nucl. Instrum. Meth. A* **849**, 112 (2017).
- [4] M. Venhart, *et al.*, *J. Phys. G* **44**, 074003 (2017).
- [5] J. Sauvage, *et al.*, *Nucl. Phys. A* **540**, 83 (1992).
- [6] S. E. Larsson, G. A. Leander, I. Ragnarsson, *Nucl. Phys. A* **307**, 189 (1978).
- [7] J. Meyer-ter-Vehn, F. S. Stephens, R. M. Diamond, *Phys. Rev. Lett.* **32**, 1383 (1974).

# Beta-decay studies

## Simulation and Calibration of the IDS charged-particle setup

Results from experiment IS633

*Sílvia Viñals, Enrique Nácher, Olof Tengblad  
for IDS, MAGISOL*

The methodology for detector calibration and energy-loss correction performed with the charged-particle spectroscopy set-up at the ISOLDE Decay Station (IDS) is presented. The characterisation of the set-up was carried out using Monte Carlo GEANT4 simulations and standard alpha-calibration sources. In this way the response function of the system is accurately determined and can be used in spectral unfolding. This work is described in detail in [3].

The experimental set-up discussed (used in IS577, IS605 and IS633 [3]), comprises of a set of four silicon  $\Delta E$ -E telescopes in “diamond” configuration mounted at the implantation point of the IDS. Each telescope is composed of a thin Double-sided Silicon Strip Detector (DSSD) backed by a silicon pad detector.

The pixel segmentation of the DSSD detectors allows the determination of the emission angle of each particle detected and thus makes it possible to accurately account for the energy lost by each particle when traversing different dead-layers. Fine tuning is achieved by tailoring the calibration for each pixel using an accurate simulation of the set-up in GEANT4. After fitting the experimental calibration spectrum per pixel, the energy detected is compared with the one obtained by the simulation for the same pixel. Then, a linear regression is carried out to obtain the linear transformation that converts the spectrum from energy per strip to energy deposited per pixel. At this point, the detector is calibrated for the energy detected in each pixel. To correct for the energy loss in the different dead-layers, a second linear transformation is applied to convert the energy deposited per pixel into the energy that would

have been detected in absence of dead-layers.

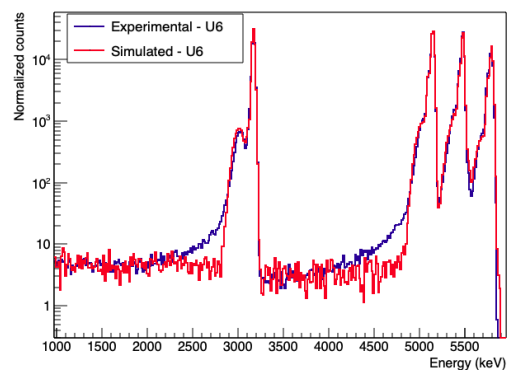


Figure 1: Comparison between the experimental calibration spectrum and the simulation of the radiation emitted by the four isotopes present in the calibration source with the geometry adjusted. DSSD 60  $\mu\text{m}$ .

The response function of a detector is defined as the pulse-height spectrum produced by a mono-energetic source. The deviation of such response from a perfect narrow peak shape is due to the finite energy resolution of the detector, incomplete energy deposition in the active volume, and incomplete charge collection in the contacts. The determination of the response function of the detector is essential for the analysis. The geometry of the set-up is thus implemented with a high level of detail in GEANT4, including all the physical/geometrical characteristics of each detector. A high reproducibility of the experimental spectrum is achieved by adjusting the thickness of the dead-layers using the response to the emission from the mono-energetic  $\alpha$ -source  $^{148}\text{Gd}$ . Once the detectors are adjusted, the other radio-isotopes present in the source were simulated and an almost perfect reproduction of the total en-

ergy spectrum is obtained Fig. 1. The non-reproduction of the tails represents less than 1%. The methodology developed here results in more accurate energy values than traditional per-strip energy calibration.

Finally, this highly detailed simulation of the set-up, and the so obtained response function of the detector at

different energies, allow us to proceed with an unfolding procedure that will soon be published.

## References

- [1] S. Viñals, *et al.*, *Eur. Phys. J. A* **57**(49) (2021).

## Determining the branching ratio of the rare $\beta$ -proton decay of $^8\text{B}$ nucleus

Results from experiment IS633

*Sílvia Viñals, Enrique Nácher, Olof Tengblad  
for IDS, MAGISOL*

The  $\beta^+$ /EC-decay of  $^8\text{B}$  mainly populates the  $2^+$  states of  $^8\text{Be}$  due to the selection rules. Decays to the  $0^+$  and  $4^+$  states are second forbidden and hence strongly suppressed. The decay to the  $1^+$  17.6 MeV state is expected to be enhanced by the proton-halo structure of  $^8\text{B}$  through EC. The  $1^+$  17.6 MeV state is situated 385 keV above the  $p + ^7\text{Li}$  threshold and, it is known from reaction studies [1], that the only decay-channel is proton emission. Following the discussion in [2], the EC decay rate can be estimated if one assumes the proton halo configuration of  $^8\text{B}$  as a  $^7\text{Be}$  core plus an orbiting proton. The EC would occur in the  $^7\text{Be}$ -core and the transition matrix element can be estimated to be the same as for the ground state of  $^7\text{Be}$  decaying into the ground state of  $^7\text{Li}$ . Scaling by the half-life, an upper limit of the branching ratio of the population of this state can be set to  $2.3 \times 10^{-8}$ .

Since the proton is emitted when the 17.6 MeV state of  $^8\text{Be}$  is populated via EC with a very low branching ratio, an anti-coincidence analysis has to be performed to remove the contribution from the  $\alpha$  particles that dominate the spectrum. Furthermore, we do not expect to observe a proton peak in the spectrum and therefore the information that will be extrapolated from this analysis is an experimental upper limit of the branching ratio. For determining this limit, a set of simulations have been performed and compared with the experimental data. In order to compare the results of the simulation with the experimental data, a large amount of statistics is needed. Due to the solid angle covered by the detectors, a total of  $10^9$   $^8\text{B}$  decays were simulated. The set-up was the IDS charged-particle setup as defined in [3] and also describe elsewhere in this Newsletter.

The validation of the simulation is done by compar-

ison between the simulated and experimental spectra. In this comparison, only the threshold curve shape is corrected in the simulated data and the more noisy strips are suppressed. In Fig 1 one can see the comparison between the anti-coincidence experimental spectrum (blue) and the same spectrum adding in grey a simulated proton peak; the proton peak is clearly visible over the background ( $N_p=2500$  over  $4\pi$ ).

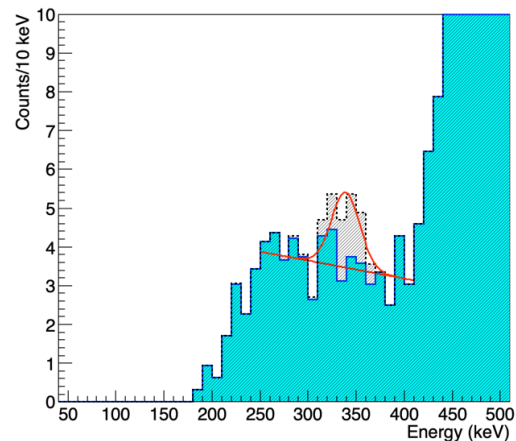


Figure 1: Comparison of the peak-shape for 2500 protons simulated where the proton peak is clearly visible over the background. In blue the anti-coincidence experimental spectrum and in grey the same spectrum when the proton peak is added.

We can thus determine the experimental upper limit to be  $2.5 \times 10^{-6}$  within a confidence level of 99.9 % ( $3\sigma$ ).

## References

- [1] R. Warner, et al., *Phys. Rev. C* **52**(3), 1160 (1995).
- [2] M. Borge, et al., *J. Phys. G* **40**, 035109 (2013).
- [3] S. Viñals, et al., *Eur. Phys. J. A* **57**(49) (2021).

## Indium Energy Spectrum Shape (InESS) at WISArD

Simon Vanlangendonck for the WISArD collaboration

The Standard Model of Particle Physics (SM) has been a great success describing three of the four fundamental interactions. At the same time, it does not resolve mysteries such as the matter-antimatter asymmetry observed in the Universe, the occurrence of dark matter and dark energy, nor the origin of CP symmetry breaking. Furthermore, the theory includes a large number of free parameters. Possible extensions referred to as Beyond Standard Model physics (BSM) are experimentally accessible through particle collisions, i.e. at LHC, or through high-precision experiments. The latter are indirect searches, and the goal of the WISArD collaboration at ISOLDE/CERN.

The WISArD experiment is being designed to measure the beta-neutrino correlation  $a_{\beta\nu}$  [1] providing access to BSM physics through the Fierz interference term  $b_F$ . Any non-zero value for this term will indicate new physics. Spectrum shape measurements can provide a complementary evaluation of the Fierz term. However electron energy measurements suffer from the backscattering effect from the detector, which deforms the observed electron energy. During LS2 we benefited from the availability of the WISArD solenoid, providing a strong magnetic field, to perform a spectrum shape measurement. We built a detector set-up with two plastic scintillators coupled to SiPMs installed face-to-face. In this configuration, the high magnetic field provides a closed system and a  $4\pi$  solid angle. Thus, adding both detector signals within an integration time window allows the reconstruction of the full electron energy.

The isotope of choice was  $^{114}\text{In}$  motivated by scientific and practical reasons. The ground state decays through a pure Gamow-Teller beta transition that is theoretically well-described [2]. Practically, its relatively long-living isomeric state ( $T_{1/2} \approx 50\text{d}$ ) and commercial availability were essential to our measurement during

LS2 and the absence of radioactive beam delivery at ISOLDE. One drawback when interested in the Fierz term for  $^{114}\text{In}$  is the lack of independent information on the nuclear structure contributions. This absence necessitates their inclusion into the spectrum fit.

At the end of 2020, we performed these types of measurements. The detector set-up was characterized, using converted electron sources ( $^{137}\text{Cs}$  and  $^{207}\text{Bi}$ ) as well as a continuous beta source ( $^{90}\text{Sr}$ ). For  $^{114}\text{In}$  two different source activities were used, i.e. 5 kBq and 1 kBq. Fig. 1 shows experimental spectra for one run obtained with the 5 kBq source. The shown events correspond to a single detector being triggered. Thus, the energy loss due to backscattering is below the energy threshold of the second detector. In these uncalibrated spectra, one sees the gain difference between both detectors. In the final analysis, a calibration procedure will be used to allow the beta energy spectrum to be fully reconstructed, including coincidence events in both detectors.

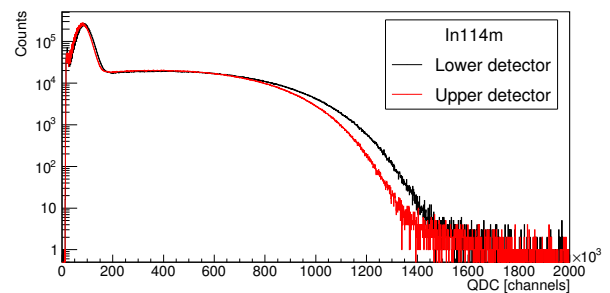


Figure 1: Spectra for one  $^{114}\text{In}$  run for both detectors. This figure includes only events with one detector triggered.

## References

- [1] V. Araujo-Escalona, *et al.*, *Phys. Rev. C* **101**, 055501 (2020).
- [2] L. Hayen, *et al.*, *Reviews of Modern Physics* **90**(1), 15008 (2018).

# Studies with post-accelerated beams

## Towards the Island of Inversion with the ISOLDE Solenoidal Spectrometer

Results of experiment IS621

David Sharp for the ISS collaboration

This year promises to be an exciting one for the ISOLDE Solenoidal Spectrometer (ISS) collaboration, with the exploitation of the device with the new Advanced Silicon Array built by the University of Liverpool. This is now installed in the magnet, as shown in Fig. 1 and is undergoing commissioning, remotely, in preparation for the HIE-ISOLDE physics campaign this year. ISS now has six proposals accepted that could potentially run this year. One of which is the study of the  $d(^{30}\text{Mg},p)^{31}\text{Mg}$  reaction, which will build on the measurement of the  $d(^{28}\text{Mg},p)^{29}\text{Mg}$  reaction made before LS2 [1]. For this measurement ISS was run in an early exploitation mode using the position-sensitive silicon array from HELIOS at Argonne National Laboratory.



Figure 1: Photo of the Liverpool advanced silicon array installed within ISS.

The excitation-energy spectrum of  $^{29}\text{Mg}$  is shown in Fig. 2 where, through a comparison of the experimental angular distributions with those calculated using the distorted-wave Born-approximation, negative-parity intruder states have been identified. The use of ISS enabled states to be probed with excellent particle resolu-

tion of  $\sim 150$  keV and enabled states both above and below the neutron-emission threshold,  $S_n$  to be studied. As strong fragments of single-particle strength for intruder states were observed above  $S_n$  this proved vital. These data provide a robust benchmark of shell-model calculations, in the last odd- $A$  magnesium isotope outside of the  $N = 20$  Island of Inversion, as well as data on the evolution of single-particle states along  $N = 17$  towards  $^{25}\text{O}$ . The results from this measurement have been submitted for publication.

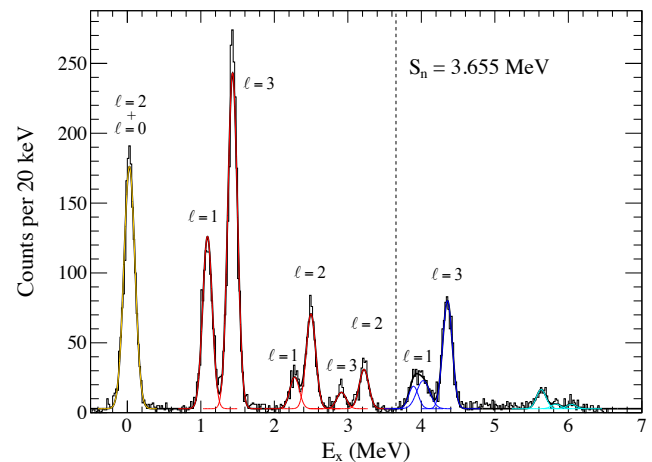


Figure 2: Excitation-energy spectrum for states populated in the  $d(^{28}\text{Mg},p)^{29}\text{Mg}$  reaction overlaid with gaussian fits to the data. The doublet of the ground and first excited state is in yellow. Resolved bound states in red. Unbound states populated in the  $^{28}\text{Mg}+n$  system are in blue and turquoise. The most probable transferred angular momentum is labelled for each state, where known.

These studies will hopefully now be extended this year in to the Island of Inversion using the  $d(^{30}\text{Mg},p)^{31}\text{Mg}$  reaction. These data, combined with the existing data, will provide systematic information on the evolution of single-particle states from outside to inside the Island of Inversion.

## References

- [1] D. K. Sharp, *et al.*, Tech. Rep. CERN-INTC-2016-030. INTC-P-470, CERN (2016).

## Coulomb excitation of $^{142}\text{Xe}$

Results of experiment IS548

Corinna Henrich for the IS548-MINIBALL collaboration

$^{142}\text{Xe}$  lies north-east of the doubly-magic  $^{132}\text{Sn}$  and only two protons below  $^{144}\text{Ba}$ , for which indications for an enhanced octupole collectivity have been reported.

To gain further understanding of the evolution of collectivity and shape in the region, a Coulomb excitation experiment was performed at HIE-ISOLDE at an energy of 4.5 MeV/u. For the detection of both the scattered beam and the recoiling target particles in coincidence with  $\gamma$  rays the particle detector array C-REX was mounted inside the  $\gamma$ -ray spectrometer MINIBALL. C-REX, an adaptation of T-REX [1] for Coulomb excitation, provides more complete angular coverage than the standard forward-facing Double-Sided Silicon-Strip Detector (DSSSD). C-REX consists of an additional set of four silicon barrel detectors under intermediate and a second DSSSD under extreme backwards angles.

The only isobaric contaminants were the daughter nuclei of the initially pure beam. The beam intensity was smaller than expected by a factor ten.

To compensate, a  $4 \frac{\text{mg}}{\text{cm}^2}$   $^{206}\text{Pb}$  secondary target was used. The drawback was a blur of the velocity distribution of the particles detected by C-REX due to straggling in the thick target.

Figure 1 shows the Doppler-corrected  $\gamma$ -ray spectra stemming from our data. The relative cross sections for the  $2^+_1$  and  $6^+_1$  states in forward and backward direction illustrate how single and multiple-step excitation processes can be distinguished in C-REX. The clean particle identification in backward direction, where the multiple-step excitation cross section is higher, provided valuable input for the interpretation.

Scarce information on the low-lying structure of  $^{142}\text{Xe}$  in conjunction with the low-statistics population of several new states turned out to make analysis very challenging. Even employing particle- $\gamma$ - $\gamma$  coincidences, from this data set alone the conclusive identification of

the new states based on the respective transitions is impossible as these are quite close to other features in the spectra. Discussions with the Osaka group analyzing  $^{142}\text{Xe}$  via  $\gamma$ -decay spectroscopy following  $\beta$  decay of  $^{142}\text{I}$  measured at RIKEN [2] were extremely important in this respect.

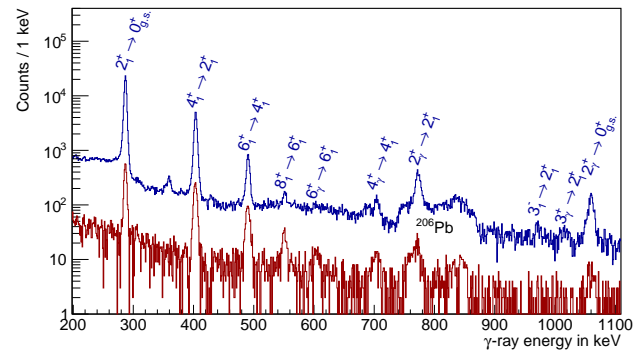


Figure 1:  $\gamma$ -ray energy-spectra Doppler corrected with respect to  $^{142}\text{Xe}$ . Particles detected in forward direction (blue) and in backward direction, barrel only (red).

The results of the analysis are the novel observation of four states interpreted as members of a  $\gamma$  band similarly to  $^{140}\text{Xe}$  [3]. Additionally, the tentative location of the  $3^-_1$  state [4] can be supported. The determined spectroscopic quadrupole moments of the lowest three yrast-band states illustrate their prolate shape, while the observed reduced transition strengths reflect their collectivity. An inconsistency of our data with the reported lifetime [5] of the  $4^+_1$  state has been found.

The experimental data is consistent with SCCM and LSSM calculations as performed by T. R. Rodríguez and H. Naïdja (private communication), respectively.

A publication is in preparation, and the doctoral dissertation resulting from this data has been published recently [6].

## References

- [1] V. Bildstein, *et al.*, *Eur. Phys. J. A* **48** (2012).
- [2] A. Yagi, *et al.*, *Accel. Prog. Rep.* **49** (2016).

[3] W. Urban, *et al.*, *Phys. Rev. C* **93**, 034326 (2016).

[4] W. Urban, *et al.*, *Eur. Phys. J. A* **16**, 303 (2003).

[5] S. Ilieva, *et al.*, *Phys. Rev. C* **94**, 034302 (2016).

[6] C. Henrich, Dissertation, TU Darmstadt (2021).

## Resonance excitations in the ${}^7\text{Be}(d,p){}^8\text{Be}^*$ reaction up to 20 MeV

Results of experiment IS554

Sk Mustak Ali, Kabita Kundalia, Dhruva Gupta  
for the IS554 collaboration

The IS554 experiment studied the resonance excitations in the  ${}^7\text{Be}(d,p){}^8\text{Be}^*$  reaction ( $Q_{gs} = 16.67$  MeV) up to about 20 MeV for the first time, in the context of the *Cosmological Lithium Problem* [1, 2]. The lithium problem is quite old and has been studied with renewed vigour in recent times [3, 4, 5, 6, 7].

We carried out this experiment at the SEC (Scattering Experiment Chamber), in the XT03 beamline of HIE-ISOLDE. A 5 MeV/A  ${}^7\text{Be}$  beam of intensity  $\sim 5 \times 10^5$  pps was incident on a 15  $\mu\text{m}$  thick  $\text{CD}_2$  target. The setup consisted of annular S3 and double-sided silicon strip detectors W1 and BB7, backed by unsegmented silicon-pad detectors. The detectors covered an angular range of  $\theta_{lab} = 8^\circ - 170^\circ$ . Runs with  $\text{CH}_2$  and  ${}^{208}\text{Pb}$  targets were also taken for background subtraction and normalization purposes respectively.

Fig. 1 shows the excitation energy spectrum of  ${}^8\text{Be}^*$  from triple coincidence of detected particles from the above reaction. The lower excitations namely 0.092, 3.03 and 11.35 MeV were obtained from the back angles, covered by the 32x32 BB7 double-sided silicon strip detectors (DSSD). In this case, we selected events with multiplicity 3, for which two hits were recorded at the forward S3 detector and one proton was detected at the BB7 DSSDs. The higher excitations of 16-20 MeV were obtained from the W1 DSSDs in the shape of a pentagon, covering  $\theta_{lab} = 40^\circ - 80^\circ$ . Here, we selected events with multiplicity 3, resulting from the detection of a proton and two  $\alpha$ -particles at W1. The counts from the W1 detectors in Fig. 1 have been multiplied by a factor of 2 for better visualization of the resonances.

At present, we are working on the angular distributions of the various excited states of  ${}^8\text{Be}^*$  and their impact on the lithium problem from the context of nuclear

physics .

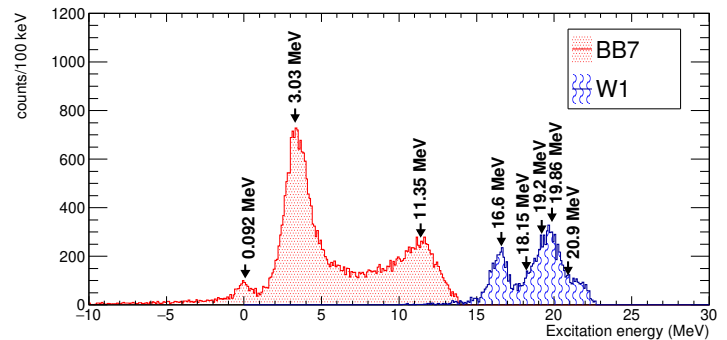


Figure 1: Excitation energy spectrum of  ${}^8\text{Be}^*$  from triple coincidence of protons and two alpha particles.

The IS554 collaboration thank the ISOLDE engineers in charge, RILIS team and Target group at CERN for their support. DG acknowledges financial support from ENSAR2 (Grant no. 654002) and ISRO, Govt. of India (Grant no. ISRO/RES/2/378/15–16).

## References

- [1] R. H. Cyburt, B. D. Fields, K. A. Olive, *Journal of Cosmology and Astroparticle Physics* **2008**(11), 012 (2008).
- [2] R. N. Boyd, C. R. Brune, G. M. Fuller, C. J. Smith, *Phys. Rev. D* **82**, 105005 (2010).
- [3] C. Angulo, *et al.*, *The Astrophysical Journal* **630**(2), L105 (2005).
- [4] N. Chakraborty, B. D. Fields, K. A. Olive, *Phys. Rev. D* **83**, 063006 (2011).
- [5] R. H. Cyburt, M. Pospelov, *Int. Jour. Mod. Phys. E* **21**(01), 1250004 (2012).
- [6] N. Rijal, *et al.*, *Phys. Rev. Lett.* **122**, 182701 (2019).
- [7] A. Inoue, *et al.*, *Journal of Physics: Conference Series* **1643**, 012049 (2020).

## Other News

### MEDICIS and MELISSA operation in 2020

MEDICIS and MELISSA

*Eric Chevallay, Charlotte Duchemin, Reinhard Heinke, Umair Khalid, Laura Lambert, Thierry Stora for the MEDICIS local team, coordination and collaboration*

From January to March 2020, MEDICIS was in technical stop mode for maintenance and upgrades. It notably included the delicate replacement of the extraction electrode and the installation of a new gas injection system in view of producing molecular beams with Chlorine. Among the technical developments, a new sample holder has been designed within the EN-STI-RBS section to facilitate the transfer of external sources produced by MEDICIS' partner institutes for transfer into our Target and ion source units after radiochemical separation. This sample holder is a tight fit, made of a tantalum cylinder with an inner part rhenium foil lining. It comes with a plexiglass protection to prevent any contamination of the transport container and to guarantee an easy and safe introduction of the boat into the oven of the target unit. All sources imported in 2020 to MEDICIS were received inside this new sample holder. Thanks to this new development, the time needed to load the source was significantly reduced, and consequently the personal exposure to radiation dose, with no incident of contamination to be reported after more than ten operations with sources from 4 partners. Another improvement of the facility was the integration of a Kromek CZT gamma-detector during the first semester of 2020, for the on-line monitoring of the collected activity during implantation onto the collection foils (see Fig. 1). The activity can now be monitored and controlled during a collection, together with the isotopic purity of the beam impinging on the foil, thanks to the quantification of specific gamma rays. This detector has already proven to significantly help with the daily opera-

tion and allowed the increase of separation efficiencies.



Figure 1: Kromek CZT gamma-detector

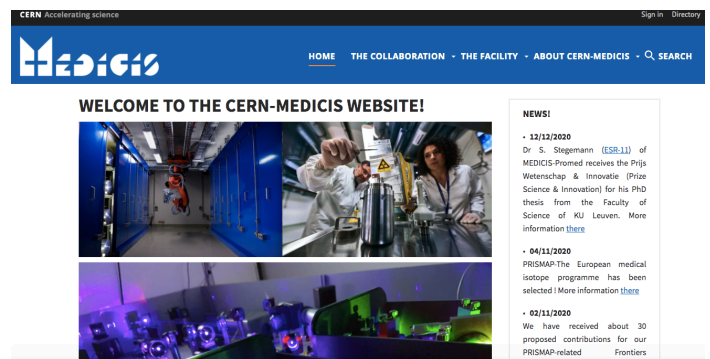


Figure 2: Welcome page of the MEDICIS website

The technical stop was followed by a successful commissioning phase with stable beams until the 16<sup>th</sup> of March 2020. From that day onwards the beam permit was suspended to put MEDICIS (as well as the full CERN accelerator complex) in safe mode due to the Covid-19 sanitary crisis. MEDICIS remained shut down for 2 months until 25<sup>th</sup> of May 2020. These two months of teleworking were used to launch the official CERN-

MEDICIS website, now available at [medicis.cern](https://medicis.cern) (see Fig. 2).

The operation of the facility restarted on 25<sup>th</sup> of May with the conditioning of the newly installed electrode at 65 kV. An additional laser (provided by JGUniversity Mainz) was received and installed at MELISSA to replace the one borrowed from RILIS. The calibration of the separator magnet was performed and 3% stable terbium separation efficiency was achieved with MELISSA. Stable samarium tests followed showing an efficiency of 31% and an optimal operation temperature around 1700 °C, which was applied and confirmed during the radioactive samarium collections. Stable thulium separation measurements were also performed, with a record efficiency of 60 to 65% achieved. Additionally, dedicated systematic measurements on the influence of high ion load on laser ionization efficiency with different elements and ion source materials were performed. In the last week of June the MEDICIS facility permit was approved and the facility received its first external radioactive source of the year on 26<sup>th</sup> of June 2020.

MEDICIS operated with radioactive ion beams from the end of June 2020 until the 9<sup>th</sup> of December 2020. A total of 17 collections were performed with 16 of them shipped to partner institutes within Europe. Four radionuclides of medical interest were collected with high specific activity: Sm-153, Tb-155, Tm-167 and Ac-225. Sm-153 had initially been produced from enriched Sm-152 targets through the (n,g) reaction at the SCK.CEN BR2 reactor (Mol, Belgium). Tb-155 was produced at Arronax (Nantes, France) from the irradiation of natural gadolinium foils with 30 MeV protons. PSI produced Tm-167 from natural erbium targets irradiated with 22.8 MeV protons. Ac-225 was provided by JRC Karlsruhe in Germany from the "milking" of a Th-229 source. Four European institutes (PSI, SCK/KU Leuven, CHUV and NPL) and five approved projects (MED-001, MED-014, MED-017, MED-024, MED-025) profited from high purity radionuclides delivered by MEDICIS in 2020. A total of 530 MBq were collected and shipped to our partners, from a total of 16.5 GBq at the beginning, resulting in an

average separation efficiency over the 2020 campaign of 3.2%. The gamma-spectrometer which is now monitoring the activity being implanted on the foils inside the collection chamber gave a maximum separated efficiency of 53.2% for Tm-167. Sputtering of the implantation layer led to a redistribution of the activity on the frame of the sample holder, leading to a figure of 22.5% in this case. This figure is deduced from the activity measured on the foil as a function of the activity which was present inside the target at the start of the collection. The two extractions of Ac-225 led to collected efficiencies of 12.5% and 9.8% respectively. The Sm-153 collection efficiencies ranged from 1.8% to 12.7% and those of Tb-155 between 1.0% and 6.1% (with a separation efficiency of 11.1% before sputtering). Important progresses for the MED-022 project, Non-invasive imaging of radioactive platinum chemotherapeutics for patient stratification, were witnessed with one gram of enriched Pt-194 procured and two test irradiations of 10 mg of metallic platinum performed with our new collaboration member, PAEC (Islamabad, Pakistan), with a successful conversion into PtCl<sub>2</sub>. A test shipment is being prepared to estimate the lead time between PAEC and Geneva.



Figure 3: Automatic radiochemistry set-up

This year radiochemistry activities restarted at MEDICIS to separate the isotopes from the zinc implantation layer. Liquid chromatography was subsequently used to separate the desired radioisotope from its isobaric contaminants. A dedicated column was developed for the separation of the collected radiolanthanides and was tested for activities of less than 1 LA (Limite d'Autorisation according to the Swiss reg-

ulation). The parameters were optimized for three radiolanthanides Sm, Tb and Tm. An automated system is being set-up in order to manipulate higher radioactivity levels above 1 LA in 2021 (see Fig. 3). Radioactive liquid concentrated acid waste has been performed to transform them into easily disposable solid waste.

Despite the global health crisis, MEDICIS developed a rich research program, with notably the first translation of high specific activity Sm-153 for theranostic applications, and achieved impressive operational performances, with Tm-167 separated at more than 50 %. On top of this, the European Medical Isotope Programme - PRISMAP, a consortium of 23 key European institutes, was selected for funding by the EC

within the H2020 Research Infrastructures INFRA-2020 program. It aims to federate European key institutes and infrastructures for the translation of emerging radionuclides into medical diagnosis and treatment as well as to promote a single hub for researchers.

*It is with great sadness that we have learnt that Gerd Beyer has passed away while this article was being written. Gerd had shown a keen interest in the MEDICIS initiative from its very first steps. In that respect, he had been a true precursor at ISOLDE, notably with Tm-167 tested for pioneer medical research, which is also focus here. Our deep condolences go to his wife and his two children.*

# ISOLDE support

## Access and contacts

---

1. Use the online pre-registration tool<sup>1</sup> which should be launched by your team leader or deputy team leader. Once launched, the document number should be sent to Jenny Weterings who will inform the users office that the document is processed. You need to attach the following documents to the pre-registration:
  - **Home Institution Declaration<sup>2</sup> signed by your institute's administration (HR).**
  - Passport
2. When your pre-registration is accepted by the CERN users office you will receive an email telling you how to activate your CERN computer account. However, you cannot activate your CERN EDH account until you arrive at CERN and complete the registration process.
3. When you arrive at CERN go to the Users office to complete your registration (Opening hours: 08:30 - 12:30 and 14:00 — 16:00 but closed Wednesday mornings).
4. Get your CERN access card in **Building 55**
5. Follow the online mandatory CERN safety courses: safety at CERN; Radioprotection awareness, Emergency evacuation, Computer security and Covid-19.
  - If you have activated your CERN account, you can access the mandatory courses online at the web page [lms.cern.ch](https://lms.cern.ch), from your computer, inside or outside CERN.
  - If you have not activated your CERN account, there are some computers available for use without the need to log in on the first floor of building 55 (Your CERN badge will be needed in order to prove your identity).
6. Complete the following online courses available at <https://lms.cern.ch>:
  - **Electrical Safety - Awareness Course - Fundamentals**
  - **Electrical Safety - Awareness Course - Facilities**If you have not activated your CERN account see the second part of entry 5.
7. Obtain a Permanent radiation dosimeter at the Dosimetry service, located in Building 55<sup>3</sup> (Opening hours: Mon. to Fri. 08:30 — 12:00). *If you do not need the dosimeter in the following month it should be returned to the Dosimetry service at the end of your visit.* The "certificate attesting the suitability to work in CERN's radiation areas"<sup>4</sup> signed by your institute will be required.
8. Follow the practical RP safety course and Electrical Awareness Module for which you will have to

<sup>1</sup>For information see [the CERN users' office](#)

<sup>2</sup>The Home Institute Declaration should not be signed by the person nominated as your team leader.

<sup>3</sup><http://cern.ch/service-rp-dosimetry> (open only in the mornings 08:30 - 12:00).

<sup>4</sup>The certificate can be found via <http://isolde.cern/get-access-isolde-facility>

<sup>5</sup>For information about how to register see <http://isolde.cern/get-access-isolde-facility>

register in advance<sup>5</sup>. These take place on Tuesdays at the training centre (building 6959) in Prevessin; the timetable for 2021 sessions has not yet been set but will likely start in the morning and continue until early afternoon. If you do not have your own transport, you can take CERN shuttle 2 from building 500. The timetable for this is [here](#).

9. Apply for access to "ISOHALL" using ADAMS: <https://www.cern.ch/adams>. (This can be done by any member of your collaboration (typically the contact person) having an EDH account<sup>6</sup>). Access to the hall is from the Jura side via your dosimeter. Find more details about CERN User registration see the [Users Office website](#). For the latest updates on how to access the ISOLDE Hall see the [ISOLDE website](#).

New users are also requested to visit the ISOLDE User Support office while at CERN. Opening hours: Monday to Friday 08:30 - 12:30

## Contacts

### ISOLDE User Support

Jenny Weterings  
 Jennifer.Weterings@cern.ch  
 +41 22 767 5828

### Chair of the ISCC

Kieran Flanagan  
 kieran.flanagan-2@manchester.ac.uk

### Chair of the INTC

Marek Pfutzner  
 Marek.Pfutzner@fuw.edu.pl

### ISOLDE Physics Section Leader

Gerda Neyens  
 gerda.neyens@cern.ch  
 +41 22 767 5825

### ISOLDE Physics Coordinator

Karl Johnston  
 Karl.Johnston@cern.ch  
 +41 22 767 3809

### ISOLDE Technical Coordinator

Joachim Vollaire  
 Joachim.vollaire@cern.ch  
 +41 22 766 4613

### ISOLDE Deputy Technical Coordinator (with special responsibility for HIE-ISOLDE)

Erwin Siesling  
 Erwin.Siesling@cern.ch  
 +41 22 767 0926

### ISOLDE Operations Section Leader

Alberto Rodriguez  
 Alberto.Rodriguez@cern.ch  
 +41 22 767 2607

More contact information at

[ISOLDE contacts](#) and at [ISOLDE people](#).

<sup>6</sup>Eventually you can contact Jenny or the Physics coordinator.